A NOVEL RECEIVER ARCHITECTURE FOR SINGLE CARRIER NOMA TRANSMISSION IN WIDEBAND SPARSE MIMO CHANNEL

A THESIS SUBMITTED TO
THE GRADUATE SCHOOL OF NATURAL AND APPLIED SCIENCES
OF
MIDDLE EAST TECHNICAL UNIVERSITY

BY

BURAK HALIL

IN PARTIAL FULFILLMENT OF THE REQUIREMENTS
FOR
THE DEGREE OF MASTER OF SCIENCE
IN
ELECTRICAL AND ELECTRONICS ENGINEERING

DECEMBER 2019

Approval of the thesis:

A NOVEL RECEIVER ARCHITECTURE FOR SINGLE CARRIER NOMA TRANSMISSION IN WIDEBAND SPARSE MIMO CHANNEL

submitted by **BURAK HALIL** in partial fulfillment of the requirements for the degree of **Master of Science in Electrical and Electronics Engineering Department, Middle East Technical University** by,

Prof. Dr. Halil Kalıpçılar
Dean, Graduate School of **Natural and Applied Sciences** _____

Prof. Dr. İlkay Ulusoy
Head of Department, **Electrical and Electronics Engineering** _____

Assist. Prof. Dr. Gökhan Muzaffer Güvensen
Supervisor, **Electrical and Electronics Engineering, METU** _____

Examining Committee Members:

Prof. Dr. Sinan Gezici
Electrical and Electronics Engineering, Bilkent University _____

Assist. Prof. Dr. Gökhan Muzaffer Güvensen
Electrical and Electronics Engineering, METU _____

Prof. Dr. Ali Özgür Yılmaz
Electrical and Electronics Engineering, METU _____

Prof. Dr. Elif Uysal
Electrical and Electronics Engineering, METU _____

Assoc. Prof. Dr. Ayşe Melda Yüksel Turgut
Electrical and Electronics Engineering, TOBB ETÜ _____

Date:

I hereby declare that all information in this document has been obtained and presented in accordance with academic rules and ethical conduct. I also declare that, as required by these rules and conduct, I have fully cited and referenced all material and results that are not original to this work.

Name, Surname: Burak Halil

Signature :

ABSTRACT

A NOVEL RECEIVER ARCHITECTURE FOR SINGLE CARRIER NOMA TRANSMISSION IN WIDEBAND SPARSE MIMO CHANNEL

Halil, Burak
M.S., Department of Electrical and Electronics Engineering
Supervisor: Assist. Prof. Dr. Gökhan Muzaffer Güvensen

DECEMBER 2019, 61 pages

In contemporary wireless communication systems, it became necessary to provide better solutions than current communication standards because of the increasing demand for massive connectivity and throughput. Non-Orthogonal Multiple Access (NOMA) has become one of the promising candidates for fifth generation (5G) communication networks. In this thesis, Sparse Code Multiple Access (SCMA) is utilized as a single carrier NOMA technique. SCMA is a transmission protocol, in which multiple users shares same time slot simultaneously. Although for 5G networks, NOMA brings many advantages such as spectral efficiency, on the other hand it demands more complex receiver designs since users share same time-slot simultaneously unlike the current systems. In order to overcome this problem, a factor-graph based novel receiver architecture is proposed. In this thesis, firstly single tap channel is analyzed in multiuser scenario and performance of the factor-graph based receiver architecture is analyzed. Secondly, MIMO is utilized for multi-tap channel scenario. In massive MIMO case, different parts of receiver antennas can be allocated for different groups. Every group consists of users with spatially correlated multi-tap channels.

Thus, receiver massive antenna array block can serve more than one group simultaneously. In this thesis, performance of a single group is analyzed. Several antenna inputs are combined together and used as a single input of a factor-graph based message passing algorithm (MPA). Also for each user's data prediction, received signal is passed through matched filter of that user. In the proposed receiver design, output of the factor graph is processed in order to predict possible "inter symbol interference (ISI)" from other symbols and "inter chip interference (ICI)" from other time slots of the same symbol. Therefore, the lost sparsity is recovered with the help of proposed processing. The system performance is analyzed for various channels with different number of taps, antennas, constellation points, angular spread (AS) and different levels of noise figure.

Keywords: Non-Orthogonal Multiple Access (NOMA), Sparse Code Multiple Access (SCMA) , Factor Graph, MIMO, 5G

ÖZ

TEK TAŞIYICILI DİKGEN OLMAYAN ÇOKLU ERİŞİM İLETİMİNDE, GENİŞBANT SEYREK ÇOK GİRİŞLİ ÇOK ÇIKIŞLI KANAL İÇİN ÖZGÜN BİR ALICI YAPISI

Halil, Burak
Yüksek Lisans, Elektrik ve Elektronik Mühendisliği Bölümü
Tez Yöneticisi: Dr. Öğr. Üyesi. Gökhan Muzaffer Güvensen

Aralık 2019 , 61 sayfa

Güncel kablosuz haberleşme sistemlerinde, daha yüksek hız gerektiren ve çok yüksek kullanıcı sayılı ağlarda da hizmet verebilmek amacıyla günümüzde kullanılan sistemlerden daha iyi çözümler üretilme ihtiyacı doğmuştur. Diksel Olmayan Çoklu Erişim (DOÇE) 5.Nesil (5G) haberleşme sistemleri için gelecek vaat eden seçeneklerden biri olarak ortaya çıktı. Bu tezde, Ayrık Kodlu Çoklu Erişim (AKÇE) tek taşıyıcılı bir DOÇE yöntemi olarak kullanıldı. AKÇE birden çok kullanıcının aynı taşıyıcı üzerinde aynı zaman parçacığını ortak kullandığı bir sistemdir. DOÇE her ne kadar 5G sistemler için daha iyi sistem performansı ve spektral verimlilik gibi avantajlar getirse de diğer taraftan çok daha karmaşık bir alıcı yapısı gerektirmektedir. Bu problemi çözmek amacıyla faktör grafiği temelli özgün bir alıcı yapısı tasarlandı. İlk olarak, tek sekmeli kanalda tek alıcı anteni ile başarılı ölçüm yapıldı. Sonrasında çok sekmeli kanallı sistemlerin başarısı Çok Girişli Çok Çıkışlı (ÇGÇÇ) yapıdan da yararlanılarak ölçüldü. Bu senaryoda incelenen grubu, kanalları uzaysal olarak ilişkili olan kullanıcılar oluşturmaktadır. Masif ÇGÇÇ'li yapılarda antenin farklı bölgeleri

farklı grupların kullanımına ayrılarak, birden fazla gruba aynı anda servis sağlayabilir. Bu tezde bir NOMA grubunun başarısı incelendi. Her grupta bir kullanıcın gönderimini tahmin etmek amacıyla, o gruba ayrılmış antenlerin çıkışları birlikte kullanılarak alınan sinyal o grubu oluşturan kullanıcıların karşıt filtresinden geçirildi ve herbir kullanıcının faktör grafiğinde tek bir girdi olarak kullanıldı. Önerilen alıcı yapısında ayrıca yan sembol karışımları ve sembol içi karışımları yok edebilmek amacıyla faktör grafiği çıkışları tekrar analiz ederek olası karışımlar alınan sinyalden ilerlemeli bir şekilde çıkarıldı. Böylece, kaybedilen ayrıklık önerilen yöntem ile geri kazanıldı. Bu çalışma; farklı sekme sayıları, farklı alıcı anten sayıları, sembol başı gönderilen bit sayısı, açısal yayılma ve farklı gürültü seviyeleri için test edildi.

Anahtar Kelimeler: Dik Olmayan Çoklu Erişim (DOÇE), Seyrek Kodlu Çoklu Erişim (AKÇE), Faktor Grafiği, ÇGÇÇ, 5G

To My Loved Ones

ACKNOWLEDGMENTS

First of all, I would like to thank my advisor Dr. Gökhan Muzaffer Güvensen for his endless support, motivation, exemplary character and leadership during thesis progress.

Secondly, I would like to thank my mother, my father, my brother and especially my sister Büşra for their support during my thesis period and whole education career.

Thirdly, I would like to show my regards to ASELSAN AŞ., my manager and my colleagues for their support and motivations.

Fourthly, I would like to thank "The Scientific and Technological Research Council of Turkey (TUBITAK)" for financial support during my master education.

Finally, I would like to thank my close friends Hayrullah Yumuş, Faruk Yıldız, Osman Erdem, Furkan Kökdoğan, Yusuf Kartal, Emir Doğan, Deniz Doğan for their support in hardest times and good memories we shared together.

TABLE OF CONTENTS

LIST OF TABLES

TABLES

LIST OF FIGURES

FIGURES

LIST OF ABBREVIATIONS

NOMA	Non-Orthogonal Multiple Access
SCMA	Sparce Code Multiple Access
OFDM	Ortogonal Frequency Division Multiple Access
LDS	Low Density Signature
TDMA	Time Division Multiple Access
SC	Single Carrier
RE	Resource Element
FG	Factor Graph
SPA	Sum-Product Algorithm
MPA	Message Passing Algorithm
MIMO	Multiple-Input and Multiple Output
FDE	Frequency Domain Equalizer
AIR	Achievable Information Rate
ISI	Inter-Symbol Interference
ICI	Inter-Chip Interference
FFT	Fast Fourier Transform
IFFT	Inverse Fast Fourier Transform
BER	Bit Error Rate
CMF	Channel Match Filter
CSI	Channel State Information

CHAPTER 1

INTRODUCTION

1.1 Literature and Background Information

1.1.1 Conventional Multiple Access Schemes

Development in wireless communication network systems continues very rapidly. From first generation communication networks to current and future communication networks different modulation schemes are used. Although, currently used modulation schemes are considered as good solutions for requirements of the networks, in a few years these schemes will remain incapable of answering the demands of the network requirements. On the other hand, thanks to the technological development, computational capabilities of the systems are also developed so more complex schemes become possible to handle. Modern schemes are enhanced as multiple access schemes because networks should provide service for multiple users simultaneously in contemporary communication networks. Because of the rapid development in technology and exponentially increasing number of devices in a network, there is need for a scheme with better performance in terms of throughput, massive connectivity, reliability, complexity and stability. Therefore, researchers are trying to find a alternative schemes in order to provide better service for the users by using resources they have such as time, frequency. In first generation (1G) frequency division multiple access (FDMA), in second generation (2G) time division multiple access (TDMA), in third generation (3G) code division multiple access (CDMA) and in fourth generation (4G) orthogonal frequency division multiple access (OFDMA) is used. In all of these modulation schemes, different users utilize different orthogonal resources in time, frequency or code domain therefore in receiver they are separated easier. How-

ever, as it is mentioned, demand from communication networks is increasing rapidly nowadays and resources are limited so that networks cannot provide orthogonality for each user so there is a necessity for a better scheme.

1.1.2 Non-Orthogonal Multiple Access (NOMA)

A promising technology, non-orthogonal multiple accesses (NOMA) can address some of the challenges encountered in conventional modulation schemes. As opposed to the conventional orthogonal multiple access technologies, NOMA can accommodate much more users via non-orthogonal resource allocation. Therefore, NOMA systems become a very hot topic for researchers who are working in communication field. However, NOMA brings some disadvantages such as it increases complexity of decoder in receiver which is the biggest disadvantage of NOMA techniques, especially when the number of users is very high. On the contrary, it provides higher capacity and throughput so it is regarded as one of the strongest candidate for 5G and future communication network schemes [1]. There are several NOMA schemes such as Power Domain NOMA and Code Domain NOMA. In this section these schemes will be introduced.

1.1.2.1 Power Domain NOMA

In ordinary NOMA systems, multiple users can share same resource element which can be time slot, frequency carrier or spreading code. However in power domain NOMA, users are separated in power domain such that different power levels are allocated for different users. The main idea behind the Power-Domain NOMA can be explained with a scenario that includes two users. The system initially compares the channel qualities of the users, then it allocates more power to the user with worse channel condition (eg. user 1) and less power for the user with better channel condition (eg. user 2) [2]. In order to decode the received signal User 1 treats user 2's transmitted signal as a noise and processes received signal directly. On the other hand, user 2 initially performs a Successive Interference Cancellation (SIC) such that it decodes user 1's message, then as a result of this cancellation it eliminates the mes-

sage transmitted from user 1. Finally it processes the remaining signal to decode the message as it can be seen from Figure 1.1 [3].

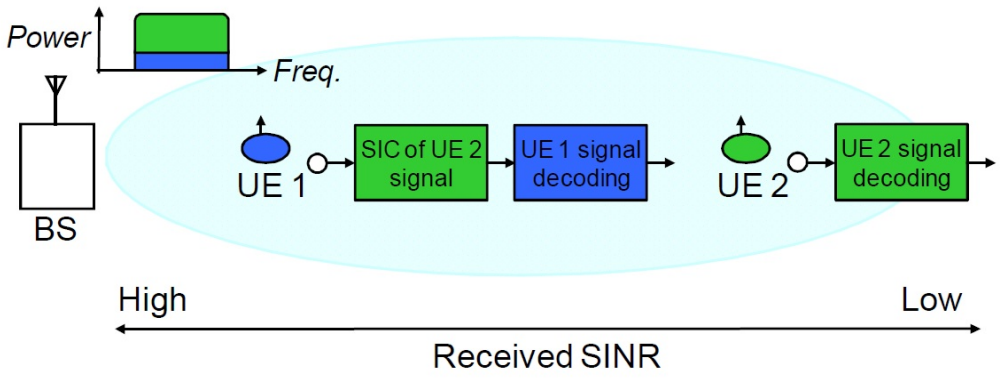

Figure 1.1: Visualization of Power Domain NOMA

1.1.2.2 Code Domain NOMA

Sparse Code Multiple Access (SCMA)

Sparse Code Multiple Access (SCMA) is another non-orthogonal multiple access method in which the information of the users are transmitted over the commonly shared resource elements such as time slot and frequency subcarrier [33]. However, the number of resource elements occupied for the single user is smaller than the total number of resource elements in the system. Therefore, there exist an overload in the system so multiple users transmit their symbols over same resource element. SCMA is an improved scheme based on Low Density Signature-Orthogonal Frequency Division Multiplexing (LDS-OFDM) that exploits sparse spreading sequences to realize overloading. Unlike LDS-OFDM, bit-to-constellation mapping and spreading with low-density signatures are combined together in SCMA. Particularly, different users' codewords are taken from different codebooks, which are generated by multidimensional constellation [4]. Sparse nature of the codebooks makes it easier to separate users signals in the receiver side. It also ensures that the number of users utilizing the same subcarrier is not too large, such that the system complexity remains manageable. Multi-dimensional codewords which are assigned to each user are sparse, therefore, in the receiver part a low-complexity message-passing algorithm (MPA) with factor

graph can decode each users' message even though they send their messages with same resource element [5]. Generally, in SCMA structures resource elements correspond to frequency subcarrier because NOMA schemes usually developed as an alternative to OFDM schemes in which orthogonal frequency subcarriers are utilized to transfer the symbols. However, in some cases resource elements can be time slots as it is utilized in this thesis.

Pattern Division Multiple Access (PDMA)

Pattern division multiple access (PDMA) is one of the novel NOMA schemes that can be realized in multiple domains. At the transmitter side, PDMA uses non-orthogonal user specific patterns which are designed to decrease the overlaps between the users' transmitted signals and increase the diversity among the users. In PDMA, multiplexing can be realized in code domain, power domain, space domain or their combinations [6]. Multiplexing strategy in PDMA is very similar to SCMA however in PDMA number of resource elements connected to the same user can be different. If multiplexing is realized in power domain, successive interference cancellation (SIC) can be used at the receiver according to signal to noise ratio of the users which are transmitting symbol. Also PDMA can utilize iterative MPA algorithm similar to SCMA.

Multiuser Shared Access (MUSA)

Multiuser Shared Access (MUSA) is one of the NOMA schemes which can is the developed version of the CDMA. As opposed to the conventional CDMA, MUSA can realize overloading by using low-correlation spreading sequences at the transmitter [4]. In MUSA scheme transmitted symbols are multiplied by the spreading sequence of the corresponding user. For a user, spreading sequence can be same for all symbols or different spreading sequence can be utilized [4]. In MUSA, after spreading process, symbols of different users are transmitted from same resource elements which are time or frequency subcarrier. For example for multi carrier scenario a symbol is transmitted during a time slot with several frequency subcarriers. Assuming that in the system there are K users and N frequency subcarriers similar to SCMA there will be an overload in the system if K is larger than N, so there will be interference of several users over the same resource element. At the receiver side, the received signal

is processed by a SIC procedure to detect each user's transmitted symbol [7].

1.1.3 Factor Graph (FG) Based Decoding via Sum-Product Algorithm (SPA)

Factor graph is a bipartite graph and it consists of two types of nodes which are factor nodes and variable nodes. Basically, factor graph represents the mathematical relation between factor nodes and variable nodes. The function node (FN) represents the signal observed at the receiving end. The variable node (VN) denotes the estimation of the signal transmitted by each user [8]. There is an edge between a factor node and a variable node only if corresponding variable node is an argument of this factor node. The edges in the factor graph are decided by the codebook design in the SCMA. In factor graph general message passing algorithm (MPA) which is also called sum product algorithm (SPA) is used in order to update factor nodes and variable nodes iteratively. Sum-product algorithm computes—either exactly or approximately—various marginal functions derived from the global function. Sum-product algorithm is utilized in lots of algorithms for years in different fields such as artificial intelligence, signal processing and digital communication [9].

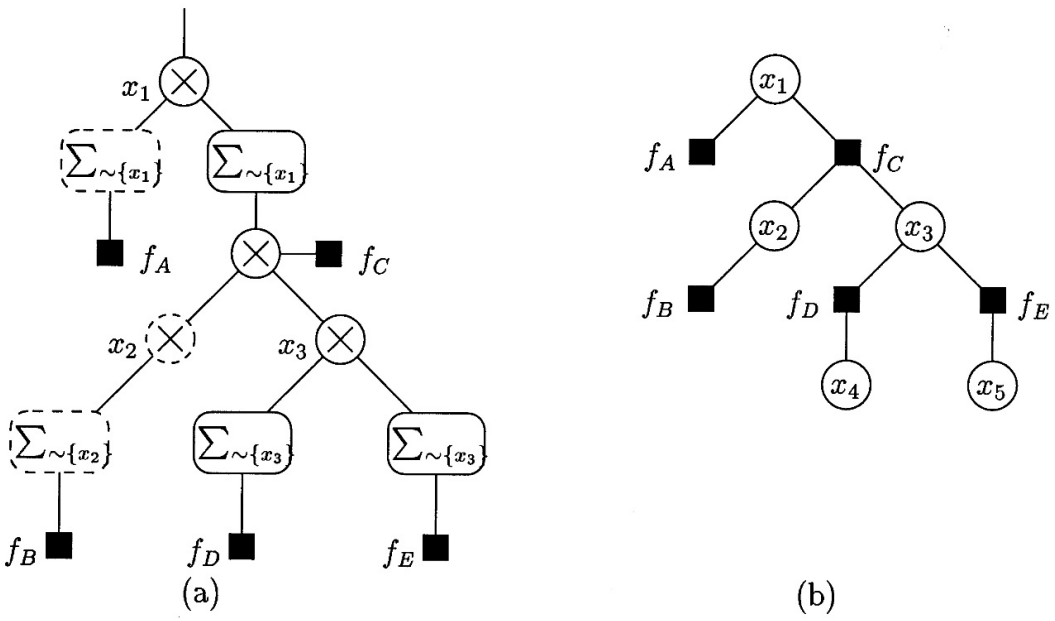

Figure 1.2: Visualization of Sum-Product Algorithm in Factor Graph

As the initial step, in factor graph, computation starts with the transmission of identity

messages from a VN to a FN over the edges connecting them. Message in the edge e which is from a VN to a FN can be calculated by the product of the messages over all the edges which are connected to this VN except edge e. On the other hand in the factor node edge e can be calculated by calculating product of received messages from its child variable nodes and then operate on the result with a $\sum_{\sim\{x_i\}}$ sum operation where $\sum_{\sim\{x_i\}}$ operation corresponds to the summation over all the variables except x_i. Visualization of this operations over arbitrary factor graph can be seen at Figure 1.2 where f_A, f_B, f_C, f_D, f_E corresponds to the factor nodes and x_1, x_2, x_3, x_4, x_5 corresponds to the vector nodes. This process is repeated for a pre-determined iteration times. Finally process for a variable node v_i is terminated by the computation of the $g_{v_i}(v_i)$ which is the product of the all the messages received in v_i. In SCMA number of FN is equal to number of resource elements and number of VN is equal to the number of users in the system. Therefore $g_{v_i}(v_i)$ corresponds to the probabilities of transmitted symbols from user i.

1.1.4 Multiple-Input and Multiple-Output (MIMO) Based Architectures

Multiple-Input and Multiple-Output (MIMO) is an architecture in which multiple antennas are used in transmitter and receiver parts. Received signals in receiver antennas are processed together in order to recover the transmitted signals. Although, MIMO systems require enhanced hardware, signal processing complexity and higher cost, using MIMO method brings lots of advantages in wireless communication systems [10]. Firstly, it increases the capacity of the communication network as well as MIMO performance of the systems by exploiting multipath propagation. On the other hand in MIMO systems higher throughput and lower BER can be achieved with the help of multiple antennas. MIMO has become an essential element of wireless communication standards including IEEE 802.11n (Wi-Fi), IEEE 802.11ac (Wi-Fi), HSPA+ (3G), WiMAX (4G), and Long Term Evolution (4G LTE)[11].

In typical MIMO systems two or four antennas are used in receiver and transmitter parts, however in massive MIMO systems number of antennas are much more than the typical MIMO scenarios. Usage of more antennas brings several advantages to the system such as systems become more resistant to jamming and interference. Besides,

massive MIMO may increase the capacity of the channel and BER performance without demanding more spectrum. In a rich scattering environment, the full advantages of the massive MIMO system can be exploited using simple beamforming strategies such as maximum ratio transmission (MRT), maximum ratio-combining (MRC) or zero forcing (ZF)[12]. In order to benefit from these advantages Channel State Information (CSI) should be known perfectly.

1.2 Motivation

Because of the dramatic developments in the technology especially in recent years, technological devices became an integral part of individuals' daily lives and as a result, data traffic of conventional devices are increased extremely. This development aroused an increase in the number of devices in the networks, their data throughput requirement from network. To illustrate, at the beginning of 2000s cellular phones were only used for simple voice conversation, nowadays cellular phones are used for video streaming, online games, social media etc. Considering that this trend will be continue, it can be foreseen that, conventional multiple schemes seems to be inadequate to fulfill the expectation of future communication networks [13][1]. On the other hand, NOMA techniques bring lots of advantages such as it improves spectral efficiency because in NOMA users can share same orthogonal resource elements which usually limits the performance of the networks. SCMA is a NOMA modulation scheme and in this scheme more than one user share resource elements as an advantage of NOMA. Moreover, due to the sparse nature of the codebooks, codebooks which are assigned for each user can be separated in receiver.

In the most of the general researches, frequency subcarriers are used as the resource element so conventional SCMA systems can be named as Multi Carrier SCMA. Main reason behind this is SCMA is assumed as an alternative to OFDM and in OFDM orthogonal frequencies are utilized. Although multi-carrier systems bring many advantages, especially in receiver part of the multicarrier systems there are some serious challenges e.g., high peak-to-average-power ratio (PAPR) [14]. Because of this reason, especially in massive MIMO systems, the use of single carrier (SC) which employs mm-wave bands, presenting sparsity both in angle and delay plane was studied

in [15], [16], [17]. As a good alternative to conventional systems single carrier SCMA is analyzed in this thesis. In this thesis a network which composes of several groups of users is studied. Every group consists of users with spatially correlated channels and proposed SCMA model analyses the performance of single group with six users which have spatially correlated channels. In addition, a novel solution is proposed for single carrier SCMA with multi-tap channel which provides an alternative system for next generation network systems.

1.3 Contribution

In this thesis, as an alternative to multi-carrier transmission which is commonly focused in recent NOMA studies, equivalent system model for single carrier SCMA transmission in dispersive MIMO channel is studied. Based on conventional model, a novel receiver with frequency domain equalizer and message passing algorithm (MPA) is proposed which operates on “A Bank of Factor Graph" with an iterative decision feedback. The proposed algorithm has similar complexity with that of the conventional ones used in SCMA framework. Contributions of this thesis to the literature are as follows:

- Instead of conventional multi carrier SCMA, single carrier SCMA system is built.
- Not only single tap but also frequency selective channel models are employed in SC transmission which is the most challenging part of SCMA because it destructs the sparse nature of SCMA codebooks.
- MIMO architecture in which channels are spatially correlated and sparse both in angle and delay domain is integrated in the system that is commonly used in contemporary networks to increase performance of the system.
- Spatio-temporal processing is studied.
- A SC-Frequency domain Equalizer is used in order to provide initial predictions to the system.

- An iterative decision feedback system architecture is designed with parallel factor graphs which has similar complexity with conventional receivers and use outputs of the bank of match filters.
- Sparsity that is lost is recovered with the help of proposed processing.

1.4 The Outline of the Thesis

In this thesis, Single-Carrier SCMA which is a NOMA modulation scheme is analyzed. In first section, background information is provided and motivation for this thesis and the contribution of this thesis to the literature are given. In chapter two, system model SC-SCMA which is utilized in this thesis is explained in order to describe the systems analyzed and help readers to visualize the system. In addition, basic transmitter and receiver architectures are described. In chapter three, novel receiver architectures are given for single carrier SCMA which is the contribution of this thesis to the literature. In this section mathematical calculations are also given which are used in signal decoding in the receiver. In chapter four, Achievable Information Rate (AIR) is introduced and its utilization in our design is explained. In chapter five, results of the simulations are presented to indicate the success of novel receiver scheme compared to the conventional NOMA receiver. Finally, in chapter six, a conclusion is given about this thesis.

Notations used in thesis: In this thesis vectors are represented by bold and small letters, matrices are reprecented by bold and capital letters. Transpose and inverse of A matrix is denoted by A^T and A^{-1}. Conjugate operaration of a is represented by a^*. Convolution is denoted as $*$ symbol. Cardinality of a set M is represented by $|M|$ and euclidian distance between x and y is denoted by $\|x - y\|$.

CHAPTER 2

SYSTEM MODEL AND DESCRIPTION

2.1 System Model for Simple Single-Carrier Sparse Code Multiple Access (SC-SCMA)

In this section, the uplink system model of SC-SCMA is described. In SCMA encoder information bit streams of each single users divided in $\log_2(M)$ bits which correspond to one NOMA symbol. For example k^{th} symbol of u^{th} user can be expressed as: $I_k^{(u)} = \sum_{i=1}^{\log_2 M} b_{k,i}^{(u)} 2^{i-1}$ where $b_{k,i}^{(u)}$ corresponds i^{th} bit of symbol k for user u. In SCMA encoder these symbols are mapped into N_c dimensional codebook $\mathbf{c}_k^{(u)}$ and cardinality is $\left|\mathbf{c}_k^{(u)}\right| = M$.

$$\textbf{\textit{NOMA codeword:}} \quad \mathbf{c}_k^{(u)} \triangleq \left[c_{I_k^{(u)}}^{(u)}[0] \quad c_{I_k^{(u)}}^{(u)}[1] \quad \ldots \quad c_{I_k^{(u)}}^{(u)}[N_c - 1] \right]^T \tag{2.1}$$

where $I_k^{(u)} \in \{1, 2, 3, \quad \ldots \quad , M\}$ corresponds to k^{th} symbol of user u. Each user has different codebook map. Codebooks contain J<N_c non zero elements and $N_c - J$ zero element where N_c corresponds to number of resource elements (RE). This means that each user uses only J RE. Each user's active resource elements are different. This sparse design principle reduces the collision of different users in same RE and reduces the decoding complexity. In this thesis, complex multi-dimensional codewords are taken from the optimized codebook design study in [18],[19]. For 4 constellation point, corresponding codewords for each user can be seen at table 2.1 and corresponding block diagram can be seen at fig 2.1. In single-carrier SCMA each resource element corresponds to a time slot so each symbol can be transmitted in N_c time slot. Therefore total transmitted signal from user u which consist of T SCMA symbols can be expressed as:

User	Symbol	Time Slot 1	Time Slot 2	Time Slot 3	Time Slot 4
User 1	00	-0.635+0.461i	0.139-0.175i	0	0
	01	0.181-0.131i	0.487-0.615i	0	0
	10	-0.181+0.131i	-0.487+0.615i	0	0
	11	0.635-0.461	-0.139+0.175i	0	0
User 2	00	0.785	0	-0.181-0.131i	0
	01	-0.224	0	-0.635-0.461i	0
	10	0.224	0	0.635+0.461i	0
	11	-0.785	0	0.181+0.131i	0
User 3	00	-0.005-0.224i	0	0	-0.635+0.461i
	01	-0.019-0.784i	0	0	0.181-0.131i
	10	0.019+0.784i	0	0	-0.181+0.131i
	11	0.005+0.224i	0	0	0.635-0.461i
User 4	00	0	0.785	0.139-0.175i	0
	01	0	-0.224	0.487-0.615i	0
	10	0	0.224	-0.487+0.615i	0
	11	0	-0.785	-0.139+0.175i	0
User 5	00	0	-0.181-0.131i	0	0.785
	01	0	-0.635-0.461i	0	-0.224
	10	0	0.635+0.461i	0	0.224
	11	0	0.181+0.131i	0	-0.785
User 6	00	0	0	0.785	-0.005-0.224i
	01	0	0	-0.224	-0.019-0.784i
	10	0	0	0.224	0.019+0.784i
	11	0	0	-0.785	0.005+0.224i

Table 2.1: SCMA Codebook

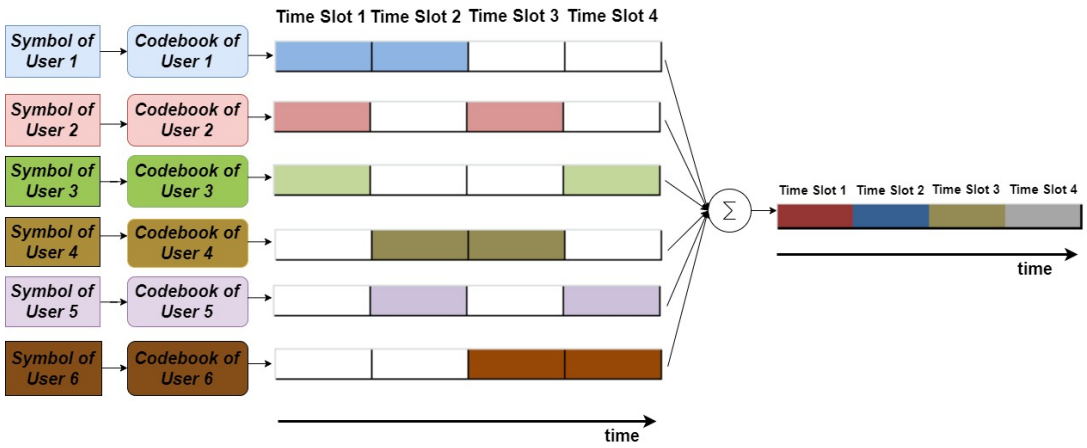

Figure 2.1: SCMA Transmitted Codewords Diagram

$$x_u[n] = \sum_{k=0}^{T-1} c^{(u)}_{I^{(u)}_k}[n - kN_c] \tag{2.2}$$

where $x_u[n]$ is the transmitted sequence for u^{th} user and $\left\{ c^{(u)}_{I^{(u)}_k}[n] \right\}_{n=0}^{N_c-1}$ is the corresponding discrete time NOMA waveform with the length N_c. In this thesis, our system model is based on a network with 6 Users and users share 4 resource element. For one symbol, each user transmits related signal in two resource elements, for corresponding symbol according to factor graph matrix F. An example for factor graph matrix with 6 users and 4 resources elements is following:

$$\mathbf{F} = \begin{bmatrix} 1 & 1 & 1 & 0 & 0 & 0 \\ 1 & 0 & 0 & 1 & 1 & 0 \\ 0 & 1 & 0 & 1 & 0 & 1 \\ 0 & 0 & 1 & 0 & 1 & 1 \end{bmatrix}$$

where $F_{i,j} = 1$ means that the j^{th} user can use the i^{th} subcarrier, and $F_{i,j} = 0$ means that this user cannot use the subcarrier $F_{i,j} = 1$ means j^{th} user can use i^{th} resource element and $F_{i,j} = 0$ means j^{th} user cannot use ith resource element Therefore during one resource element 3 user transmit active signal. In addition, because of the fact that each user has different active resource elements group in receiver they can be reconstructed by using factor graph. In this system, constellation points for each user, which are transmitted in active resource elements of this user, are selected from 4 dimensional complex codewords of codebook. Therefore 4 dimensional codewords

are sparse vector with $2 < 4$ non-zero entries [20]. In single tap simple channel the received signal in receiver can be expressed as:

$$r[n] = \sum_{u=1}^{K} h_u x_u[n] + n[n] \tag{2.3}$$

where $h_u[n]$ is Rayleigh channel coefficients for user u, $n[n]$ is the noise figure in the channel.

2.2 Wideband Sparse Frequency Selective MIMO Channel Model for Single-Carrier NOMA Transmission

In frequency selective MIMO channel model as opposed to the simple channel, channels between receiver and transmitter is multi-tap channel with L tap with ζ active taps. In receiver there are N receiver antenna. Therefore the received signal can be expressed as:

$$\mathbf{r}[n] = \sum_{u=1}^{K} \mathbf{h}_u[n] * x_u[n] + \mathbf{n}[n] \tag{2.4}$$

In MIMO multi-tap channel, channel coefficients $\mathbf{h}_u[n]$ are calculated from auto-covariance function.

In this work users are assumed to be close enough hence the center degrees of received signals are assumed same for each user. Also, the power of multipath components are concentrated in an angular spread. Auto-covariance matrix can be calculated as [14]:

$$\mathbf{R}_l^{(u)} = \int_{(\mu_l^u)-\frac{\Delta_l^{(u)}}{2}}^{(\mu_l^u)+\frac{\Delta_l^{(u)}}{2}} \rho_l(\phi)\mathbf{u}(\phi)\mathbf{u}^H(\phi)\, d\phi \tag{2.5}$$

where $\mu_l^{(u)}$ corresponds to center degree of l^{th} active tap of user u, $\Delta_l^{(u)}$ corresponds to the angular spread (AS) of l^{th} active multipath component of u^{th} user and $\rho_l(\phi)$ is the power-angle delay profile which is a positive constant only in an small interval $[\mu_l^u - \frac{\Delta_l^{(u)}}{2}, \mu_l^u + \frac{\Delta_l^{(u)}}{2}]$ for l^{th} such that $\sum_{l=1}^{N} trace\left(\mathbf{R}_l^{(u)}\right) = 1$.

$$\mathbf{u}\left(\phi\right) = \frac{1}{\sqrt{N}}\left[1, e^{j\pi sin(\phi)}, ..., e^{j\pi(N-1)sin(\phi)}\right]^T \qquad \text{where} \quad \frac{-\pi}{4} < \phi < \frac{\pi}{4} \tag{2.6}$$

Firstly, number of active taps between total channel taps are decided as can be seen from Figure 2.2;

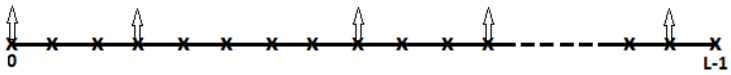

Figure 2.2: MULTI-TAP ACTIVE TAPS DIAGRAM

By using this auto-correlation matrix channel coefficients are calculated as;

$$\mathbf{h}_u[l] \sim CN(0, R_l^{(u)}) \tag{2.7}$$

Received signal in antenna array $\mathbf{r}[n]$ can be expressed as:

$$\mathbf{r}[n] = \sum_{u=1}^{K} \mathbf{h}_u[n] * x_u[n] + n[n] \tag{2.8}$$

2.3 Equivalent Discrete Time Model for Factor Graph Implementation with Bank of Channel Match Filter

2.3.1 Single Tap Channel with Single Receiver Antenna Scenario

In this scenario, each user transmits its corresponding SCMA codeword in a Rayleigh Channel and it receives using a single receiver antenna and this received signal directly processed in factor graph. This model is simpler because of the fact that there is no multipath effects in the system. This reduces the receiver complexity because there is no Inter-Symbol Interference (ISI) which is arises from other SCMA codewords and Inter-Chip Interference (ICI) which is arises from the other chips of the same codeword. Hence, sparse nature of the system is not corrupted. Therefore, this signal can be directly used as the input of factor graph and factor graph can separate users' signal without any additional effort. Block diagram of this model can be seen at Figure 2.3

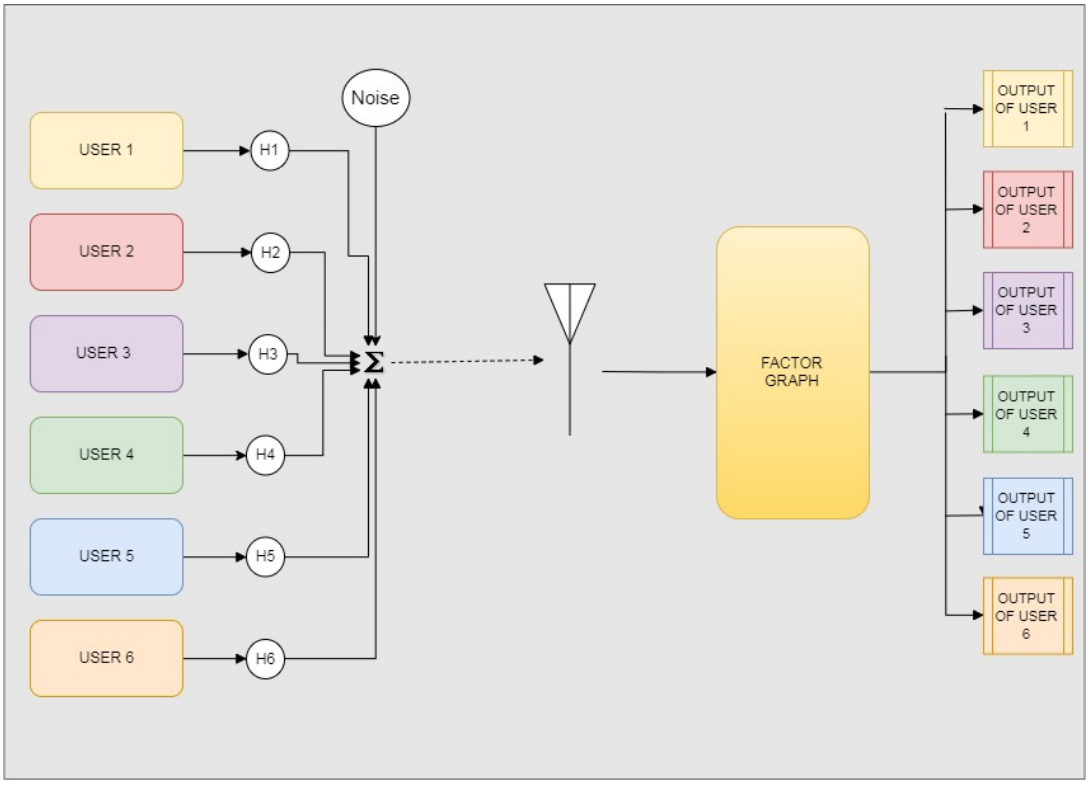

Figure 2.3: Basic Factor Graph Receiver for Single-Tap Channel

2.3.2 Multi Tap Channel with Single Receiver Antenna Scenario

In multi tap channel with single receiver antenna scenario channel, performance of the factor graph is analyzed in a channel with multipath. Therefore ISI and ICI become an important factor in the performance. In order to diminish the performance loss of the system a new receiver system is designed and in this new system received signal passed through the matched filter for each user separately.

$$y_u[n] = h_u^*[-n] * r[n] = \sum_{l=0}^{L-1} h_u^*[l] r[n+l] \tag{2.9}$$

where h_u^* is the channel match filter of user u which is conjugate of h_u^H and $y_u[n]$ is the output of CMF of user u which will be used in factor graph which is assigned to decode user u. Then, the outputs of the match filter are processed by factor graph. This means that $K = 6$ factor graph is processed in parallel and decision of corresponding user is acquired from this user's factor graph. Finally by combining the outputs of factor graphs for each user total predictions are attained. Block diagram of this model can be seen at Figure 2.4

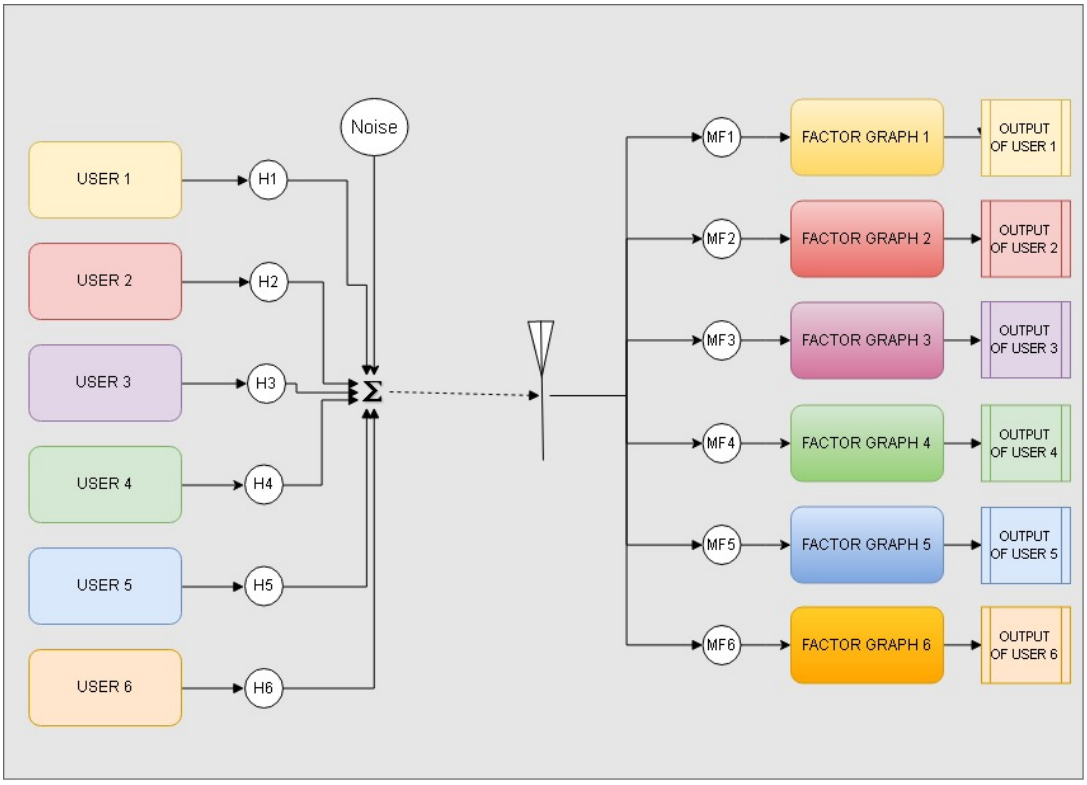

Figure 2.4: Factor Graph Receiver for Multi-Tap Single Antenna Channel

2.3.3 Multi Tap Channel with Multiple Receiver Antenna Scenario

In multi-tap channel with multiple receiver antenna scenario MIMO is integrated in the system. In receiver, multiple antennas are utilized so that more reliable signals are extracted in receiver part. Received signal $\mathbf{r}[n]$ is passed through the corresponding channel match filter for each user so input signal for factor graph for user u $y_u[n]$ can be calculated as:

$$y_u[n] = \mathbf{h}_u^H[-n] * \mathbf{r}[n] = \sum_{l=0}^{L-1} \mathbf{h}_u^H[l]\mathbf{r}[n+l] \tag{2.10}$$

where $\mathbf{r}_u^H[n]$ is the channel match filter of user u which corresponds to the complex conjugate transpose of $\mathbf{r}_u[n]$. In MIMO case $y_u[n]$ can be also expressed as:

$$
\begin{aligned}
y_u[n] &= \mathbf{h}_u^H[-n] * \left(\sum_{k=1}^{K} \mathbf{h}_k[n] * x_k[n] + \mathbf{n}[n] \right) \\
&= \sum_{k=1}^{K} \mathbf{h}_u^H[-n] * \mathbf{h}_k[n] * x_k[n] + \mathbf{h}_u^H[-n] * \mathbf{n}[n] \\
&= \sum_{k=1}^{K} p_{(u,k)}[n] * x_k[n] + n_u[n] \qquad (2.11)
\end{aligned}
$$

where, $n_u[n] = \mathbf{h}_u^H[-n] * \mathbf{n}[n]$ and $p_{(u,k)}[n] \triangleq \mathbf{h}_u^H[-n] * \mathbf{h}_k[n]$. $p_{(u,k)}[n]$ is cross channel match filter output of user u and user k In this scenario two different cases are analyzed. In the first case, users are assumed to be separated enough and therefore channels of the users are orthogonal and in the second case, users are assumed to be close enough so their active multi-taps and the center degrees of received signals are the same. Block diagram of this model can be seen at Figure 2.5

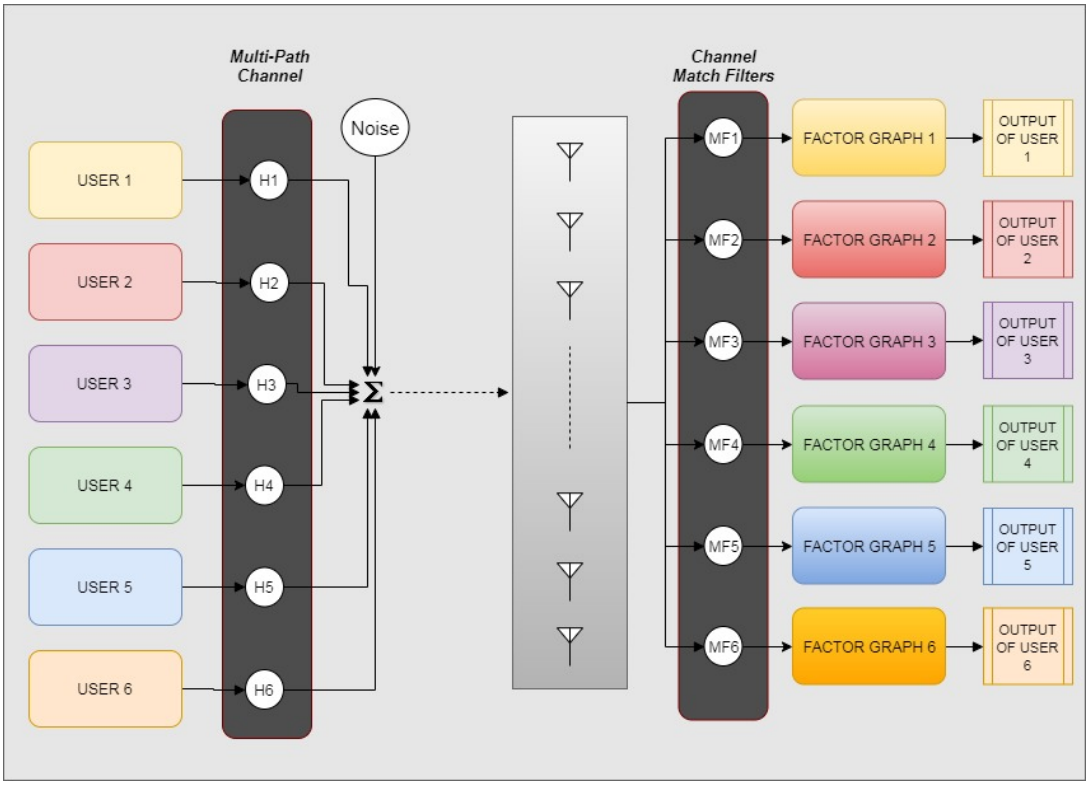

Figure 2.5: Factor Graph Receiver for Multi-Tap MIMO Architecture

CHAPTER 3

REDUCED COMPLEXITY RECEIVER STRUCTURES FOR UPLINK SINGLE-CARRIER NOMA TRANSMISSION

3.1 Conventional Structures

In order to show the performance improvement of the proposed novel receiver over conventional receiver structures, conventional receiver structures are implemented as the initial step. These conventional SCMA receiver schemes not only used as performance benchmark but also the output of conventional decoder structures are utilized in novel receiver architecture in order to provide a-priori predictions for transmitted symbols.

3.1.1 Single User ML Decoding

Single user ML Decoder is implemented in order to show the poor performance of the simple receiver in non-orthogonal multiple access schemes even in channels with high SNR. The main reason of this low performance is that in SCMA more than one user shares a resource element simultaneously and separation of the symbols of each user requires more complex receiver architectures. The performance of single user ML-decoding structure is analyzed in single tap channel, multi tap channel, single receiver antenna design and multiple receiver antenna design.

For example in multi-tap channel with multiple receiver antenna scenario, each user transmits their messages in multi-tap channel and corresponding signal $\mathbf{r}[n]$ is re-

ceived in MIMO antennas where

$$\mathbf{r}[n] = \sum_{u=1}^{K} \mathbf{h}_u[n] * x_u[n] + \mathbf{n}[n] \tag{3.1}$$

Received signal $\mathbf{r}[n]$ is passed through channel match filter (CMF) of each user separately and y_u which is input signal of the ML estimation for user u is acquired.

$$y_u[n] = \mathbf{h}_u^H[-n] * \mathbf{r}[n] = \sum_{l=0}^{L-1} \mathbf{h}_u^H[l]\mathbf{r}[n+l] \tag{3.2}$$

where $\mathbf{h}_u^H[n]$ is the channel match filter of user u

Then for each user symbol-wise ML Estimation is used. Basically, ML estimator make its symbol predictions by calculating norm distances between output of channel math filter and each possible transmitted codeword from corresponding $\mathbf{c}_k^{(u)}$ from users where

$$\mathbf{c}_k^{(u)} \triangleq \begin{bmatrix} c_{I_k^{(u)}}^{(u)}[0] & c_{I_k^{(u)}}^{(u)}[1] & \dots & c_{I_k^{(u)}}^{(u)}[N_c-1] \end{bmatrix}^T \tag{3.3}$$

$I_k^{(u)} \in \{1, 2, 3, \quad \dots \quad, M\}$ corresponds to k'th symbol of user u. And $\mathbf{c}_k^{(u)}$ codeword transmitted for symbol k of user u $I_k^{(u)}$.

For u^{th} user's k^{th} symbol corresponding received signal which will be used in ML estimator can be written as:

$$\mathbf{z}_k^{(u)} = \begin{bmatrix} y_u[kN_c] & y_u[kN_c+1] & \dots & y_u[kN_c+N_c-1] \end{bmatrix}^T \tag{3.4}$$

In ML estimator in order to make a simpler estimation cross channel coefficients assumed to be perfect where cross channel coefficients between user $u1$ and user $u2$ can be expressed as:

$$p_{(u1,u2)}[n] \triangleq \mathbf{h}_{u1}^H[-n] * \mathbf{h}_{u2}[n] \tag{3.5}$$

Therefore, in our design ML estimator in which multiuser interference ve intersymbol interference are ignored for the transmitted symbol estimation for k^{th} symbol of user u $\hat{I}_k^{(u)}$ can be written as:

$$\text{Single User ML Detector:} \quad \hat{I}_k^{(u)} = \underset{I_k^{(u)}}{\operatorname{argmin}} \left\| \mathbf{z}_k^{(u)} - p_{(u,u)}[0]\mathbf{c}_k^{(u)} \right\|^2 \tag{3.6}$$

3.1.2 Single User ML Decoding with Single-Carrier Frequency Domain Equalizer (SC-FDE)

In order to increase the performance of the novel receiver a single carrier frequency domain equalizer is implemented. Equalizers are commonly used in communication networks which mainly reverse the distortion incurred by a signal transmitted through a channel. In digital communication main purpose of the equalizers is to reduce inter symbol interference to allow recovery of the transmit symbols for frequency selective channels. In this novel receiver architecture, frequency domain equalizer is utilized because the network resides in a multipath channel which causes ISI and destruct the received signal. In this architecture, transmitted signals are received in receiver antennas and firstly processed in SC-FDE. In novel receiver architecture, the outputs of the equalizer are used to calculate possible ICI and ISI in the received signal and they are canceled from received signal. The outputs of SC-FDE are utilized in the novel receiver and improvement in BER performance of the system is observed by comparing the performance of the system with SC-FDE and without SC-FDE. SC-FDE design can be seen at Figure 3.1:

In frequency domain equalizer design, first of all for a channel with L tap, as a cycle prefix, transmitted signals of each user during last $L-1$ time slot is inserted to the beginning of the signal [21]. In FDE, Received signal $\mathbf{r}$ in antenna array can be expressed as:

$$\begin{bmatrix} \mathbf{r}[0] \\ \mathbf{r}[1] \\ \mathbf{r}[2] \\ \vdots \\ \mathbf{r}[T^{'}-1] \end{bmatrix} = \begin{bmatrix} \mathbf{H}[0] & 0 & \dots & \mathbf{H}[2] & \mathbf{H}[1] \\ \mathbf{H}[1] & \mathbf{H}[0] & \dots & \mathbf{H}[3] & \mathbf{H}[2] \\ \mathbf{H}[2] & \mathbf{H}[1] & \dots & \mathbf{H}[4] & \mathbf{H}[3] \\ \vdots & \vdots & \dots & \ddots & \vdots \\ 0 & 0 & \dots & \mathbf{H}[1] & \mathbf{H}[0] \end{bmatrix} \begin{bmatrix} \mathbf{x}[0] \\ \mathbf{x}[1] \\ \mathbf{x}[2] \\ \vdots \\ \mathbf{x}[T^{'}-1] \end{bmatrix} \tag{3.7}$$

where $T^{'} = TN_c$ is total time slot of transmitted signals, $\mathbf{r}[n] = [r_1[n] \quad r_2[n]...r_N[n]]^T$ is received signal in antenna array for n^{th} time slot in system with N receiver antenna, $\mathbf{x}[n] = [x_1[n] \quad x_2[n]...x_K[n]]^T$ where $x_u[n]$ is the transmitted signal from user u in n^{th} time slot, $\mathbf{H}[n] = [\mathbf{h}_1[n] \quad \mathbf{h}_2[n] \quad \mathbf{h}_3[n] \quad ... \quad \mathbf{h}_K[n]]$ is the channel's l^{th} tap co-

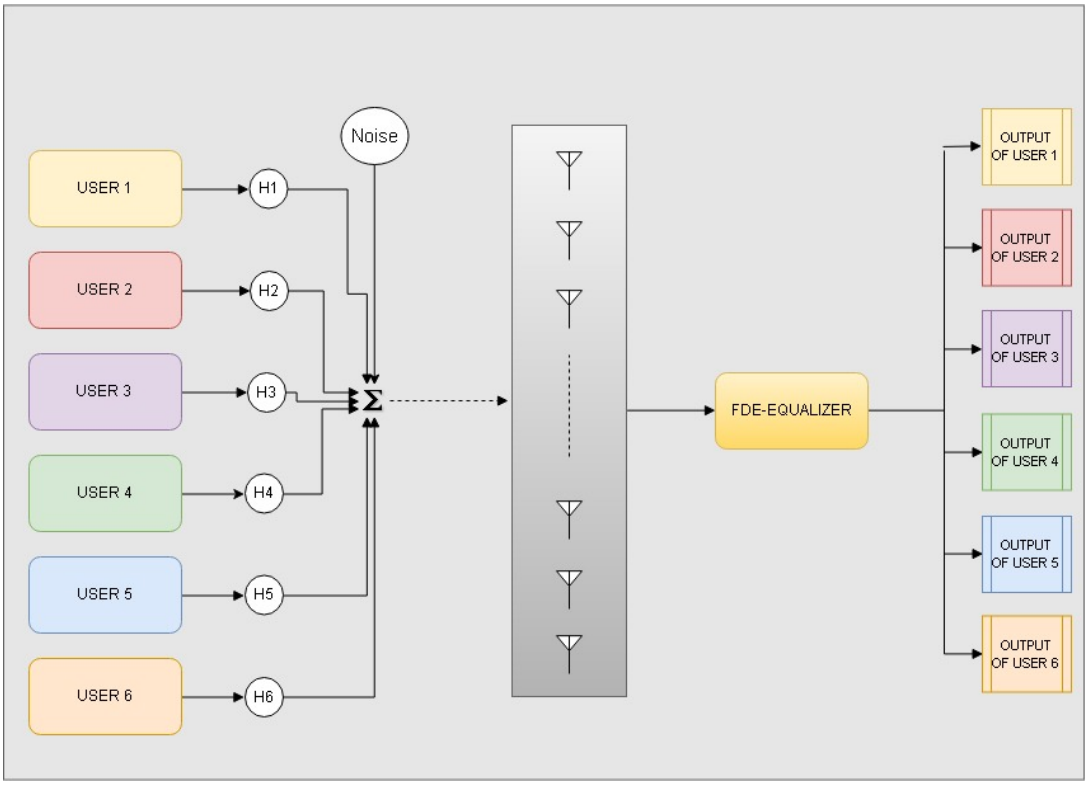

Figure 3.1: SC-FDE Diagram

efficient for system with K transmitter user. And $\mathbf{H}[n]$ can be also expressed as:

$$\mathbf{H}[n] = \begin{bmatrix} h_1^1[n] & h_2^1[n] & \dots & h_K^1[n] \\ h_1^2[n] & h_2^2[n] & \dots & h_K^2[n] \\ h_1^3[n] & h_2^3[n] & \dots & h_K^3[n] \\ \vdots & \vdots & \dots & \vdots \\ h_1^N[n] & h_2^N[n] & \dots & h_K^N[n] \end{bmatrix} \tag{3.8}$$

where $h_u^k[n]$ is the channel coefficient between k^{th} antenna of u^{th} user for n^{th} tap index. Then H matrix can be also written as:

$$\mathbf{H} = (\mathbf{Q} \otimes \mathbf{I}_N) \quad blockdiag\{\mathbf{\Lambda}_n\}_{n=0}^{T'-1} \quad \left(\mathbf{Q}^H \otimes \mathbf{I}_K\right) \tag{3.9}$$

where $\otimes$ is the Kronecker product operation and Q is $T^{'}xT^{'}$ DFT Matrix. Elements of the DFT Matrix can be calculated as $Q_{(m,n)} = \frac{1}{\sqrt{T'}} e^{j\frac{2\pi mn}{T'}}$ where m is the row number

and n is the column number. $blockdiag\{\mathbf{\Lambda}_n\}_{n=0}^{T^{'}}$ can be shown as:

$$blockdiag\{\mathbf{\Lambda}_n\}_{n=0}^{T'-1} = \begin{bmatrix} \mathbf{\Lambda}_0 & \mathbf{0} & \mathbf{0} & \mathbf{0} & \dots & \mathbf{0} \\ \mathbf{0} & \mathbf{\Lambda}_1 & \mathbf{0} & \mathbf{0} & \dots & \mathbf{0} \\ \mathbf{0} & \mathbf{0} & \mathbf{\Lambda}_2 & \mathbf{0} & \dots & \mathbf{0} \\ \vdots & \vdots & \vdots & \vdots & \dots & \vdots \\ \mathbf{0} & \mathbf{0} & \mathbf{0} & \mathbf{0} & \dots & \mathbf{\Lambda}_{T'} \end{bmatrix} \tag{3.10}$$

Each $\mathbf{\Lambda}_n$ is NxK matrix and their elements can be calculated as $\Lambda_n = \sum_{l=0}^{L-1} \mathbf{H}[l].e^{-j\frac{2\pi}{T'}ln}$ where $n = 0, 1, ..., T' - 1$ which corresponds to T' point DFT of $\{\mathbf{H}[l]\}_{l=0}^{T'-1}$.

So our equation (3.7) can be converted to:

$$\left(\mathbf{Q}^H \otimes \mathbf{I}_N\right) \begin{bmatrix} \mathbf{r}[0] \\ \mathbf{r}[1] \\ \mathbf{r}[2] \\ \vdots \\ \mathbf{r}[T^{'}] \end{bmatrix} = \begin{bmatrix} \mathbf{\Lambda}_0 & \mathbf{0} & \mathbf{0} & \mathbf{0} & \dots & \mathbf{0} \\ \mathbf{0} & \mathbf{\Lambda}_1 & \mathbf{0} & \mathbf{0} & \dots & \mathbf{0} \\ \mathbf{0} & \mathbf{0} & \mathbf{\Lambda}_2 & \mathbf{0} & \dots & \mathbf{0} \\ \vdots & \vdots & \vdots & \vdots & \dots & \vdots \\ \mathbf{0} & \mathbf{0} & \mathbf{0} & \mathbf{0} & \dots & \mathbf{\Lambda}_{T'} \end{bmatrix} \left(\mathbf{Q}^H \otimes \mathbf{I}_K\right) \begin{bmatrix} \mathbf{x}[0] \\ \mathbf{x}[1] \\ \mathbf{x}[2] \\ \vdots \\ \mathbf{x}[T^{'}] \end{bmatrix} \tag{3.11}$$

As mentioned before Q is $T^{'}xT^{'}$ DFT Matrix so equation 3.11 can be represented as:

$$\mathbf{r}_f = blockdiag\{\mathbf{\Lambda}_n\}_{n=0}^{T^{'}-1}\mathbf{x}_f + \mathbf{n} \tag{3.12}$$

where $\mathbf{r}_f$ is DFT of $\mathbf{r}$ and $\mathbf{x}_f$ is is DFT of $\mathbf{x}$. Therefore equation is transferred to the frequency domain. Also this equation can be written as:

$$\mathbf{r}_f[n] = \mathbf{\Lambda}_n\mathbf{x}_f[n] + \mathbf{n}_f[n] \tag{3.13}$$

where $n = 0, 1, 2, ..., TN_c - 1$. Also, $\hat{\mathbf{x}}_{f,n}$ can be calculated as:

$$\hat{\mathbf{x}}_f[n] = \left(\mathbf{\Lambda}_n^H\mathbf{\Lambda}_n + \frac{N_0}{Es}\mathbf{I}_{KxK}\right)^{-1}\mathbf{\Lambda}_n^H\mathbf{r}_f[n] \tag{3.14}$$

where $\frac{Es}{N_0}$ is the SCMA symbol power and $\mathbf{\Lambda}_n^H$ is the conjugate transpose of $\mathbf{\Lambda}_n$ and $\left(\mathbf{\Lambda}_n^H\mathbf{\Lambda}_n + \frac{N_0}{Es}\mathbf{I}_{KxK}\right)^{-1}$ is the matrix inverse of the $\mathbf{\Lambda}_n$ and $\left(\mathbf{\Lambda}_n^H\mathbf{\Lambda}_n + \frac{N_0}{Es}\mathbf{I}_{KxK}\right)$. Thus

by calculating IFFT of the $\hat{\mathbf{x}}_f$ we can get the output of Single-Carrier-Frequency Domain Equalizer design $\hat{\mathbf{x}}$.

$$\hat{\mathbf{x}}[n] = \frac{1}{\sqrt{T'}} \sum_{k=0}^{T'-1} \hat{\mathbf{x}}[k] e^{\frac{j2\pi kn}{T'}} \tag{3.15}$$

which corresponds to IDFT operatipn in temporal domain. From output $\hat{\mathbf{x}}$ estimations for each NOMA symbol transmitted from each user is calculated in that way:

$$\hat{\mathbf{z}}_k^{(u)} = [\mathbf{e}_u^H \hat{\mathbf{x}}[kN_c] \quad \mathbf{e}_u^H \hat{\mathbf{x}}[kN_c+1] \quad \mathbf{e}_u^H \hat{\mathbf{x}}[kN_c+2] \quad ... \quad \mathbf{e}_u^H \hat{\mathbf{x}}[kN_c+N_c-1]]^T \tag{3.16}$$

where $\hat{\mathbf{z}}_k^{(u)}$ is the output of the equalizer which corresponds to the k^{th} transmitted codeword from user u as k^{th} NOMA symbol where $k = 0, 1, 2, ..., T$, e_u is the basis vector and can be expressed as: $e_u = [0 \quad 0...0 \quad 1 \quad 0...0 \quad 0]^T$ which has only non-zero element in u^{th} index, and $\hat{\mathbf{x}}[i] = [\hat{x}_1[i] \quad \hat{x}_2[i] \quad ... \quad \hat{x}_K[i]]^T$ Finally, transmitted NOMA symbols from every user are estimated from a ML estimator which can be written as:

$$\text{ML detector:} \quad \hat{I}_k^{(u)} = \underset{I_k^{(u)}}{\operatorname{argmin}} \left\| \hat{\mathbf{z}}_k^{(u)} - \mathbf{c}_k^{(u)} \right\|^2 \tag{3.17}$$

where $\mathbf{c}_k^{(u)} \triangleq \left[c_{I_k^{(u)}}^{(u)}[0] \quad c_{I_k^{(u)}}^{(u)}[1] \quad ... \quad c_{I_k^{(u)}}^{(u)}[N_c-1] \right]^T$ and $I_k^{(u)} \in \{1, 2, 3, \quad ... \quad , M\}$ corresponds to k'th symbol of user u. And $\mathbf{c}_k^{(u)}$ codeword transmitted for symbol k of user u $I_k^{(u)}$

3.2 Conventional SCMA Decoder

In this thesis, novel receiver architecture for Single Carrier NOMA is designed and as it is mentioned in system model; mainly three different models are analyzed. In the first design, which is mentioned in section 2.3.1, a basic single carrier model in a single tap channel with single receiver antenna is analyzed in order to test the performance of the NOMA in single carrier SCMA schemes. In this architecture, signals are transmitted in a single tap channel. Channel is assumed to be a Rayleigh channel. Therefore, the received signal is only disturbed with a noise figure. In

conventional single tap SCMA received which is commonly studied case in literature, signal $r[n]$ for given time slot in receiver can be expressed as:

$$r[n] = \sum_{u=1}^{K} h_u x_u[n] + n[n] \tag{3.18}$$

where h_u denotes the channel coefficient of user u, and $x_{(u)}[n]$ is the transmitted signal from user u. Received signal $r[n]$ is directly processed in factor graph. First of all norm difference between the received signal $\mathbf{r}[n]$ and every single combination of possible transmitted signals from users which are active during selected time slot (RE) is calculated. As it can be seen from factor graph representation of the model only three users are active during any time slot. Symbol-wise representation of received signal is:

$$\mathbf{z}_k = [r[kN_c + 1] \quad r[kN_c + 1] \quad ... \quad r[kN_c + N_c - 1]]^T \tag{3.19}$$

First of all possible norm distances are calculated as:

$$\begin{aligned} d_k^w\left(I_i, I_j, I_l\right) &= -\frac{\|z_k[w] - S_1 - S_2 - S_3\|^2}{N_0} \\ S_1 &= h_i c_{I_i}^{(i)}[w] \\ S_2 &= h_j c_{I_j}^{(j)}[w] \\ S_3 &= h_l c_{I_l}^{(l)}[w] \end{aligned} \tag{3.20}$$

where $z_k[w]$ is the w^{th} index of the received NOMA symbol, $d_k^w\left(I_i, I_j, I_l\right)$ is the norm distance value between received signal in corresponding time slot and expected transmitted signals from active users i, j, l. Users i, j, l transmit the symbols I_i, I_j, I_l respectively for w^{th} time slot of k^{th} symbol. So S_1, S_2, S_3 corresponds to the possible transmitted signals from each of the active three user during time slot w. h_i is channel coefficient for user i and $c_{m_i}^{(i)}$ is the transmitted codeword from user i for symbol I_i during corresponding time slot.

$$\mathbf{c}_{I_i}^{(i)} \triangleq \left[c_{I_i}^{(i)}[0] \quad c_{I_i}^{(i)}[1] \quad ... \quad c_{I_i}^{(i)}[N_c - 1]\right]^T \tag{3.21}$$

$$\phi_k^w\left(m_i, m_j, m_l\right) = exp\left\{d_k^w\left(m_i, m_j, m_l\right)\right\} \tag{3.22}$$

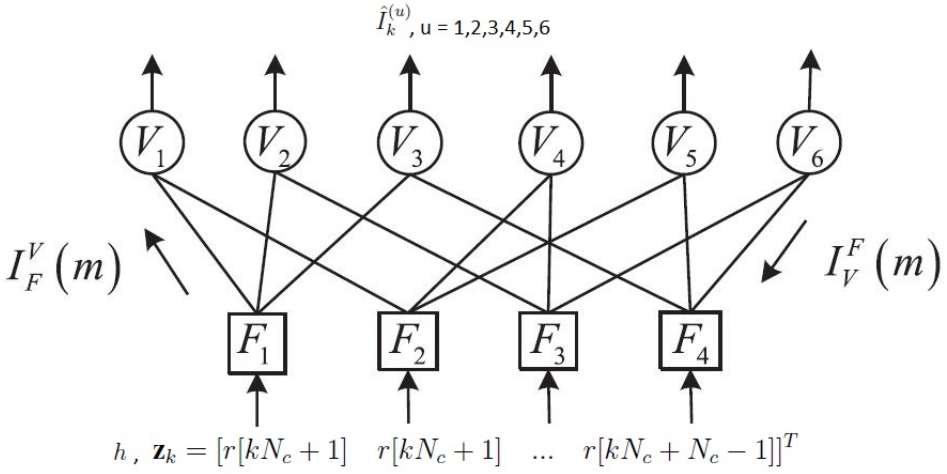

Figure 3.2: Factor Graph Representation for SCMA with K = 6 and #RE = 4

Then in graph of this structure, Factor Nodes and Vector Nodes of the message passing algorithm (MPA) are updated in an iterative manner respectively [22] the update rule of the nodes can be written as ;

$$I_{F_n}^{V_i}(m_i) = \sum_{m_j=0}^{M-1} \sum_{m_k=0}^{M-1} I_{V_j}^{F_n}(m_j).I_{V_k}^{F_n}(m_k).\phi_k^w(m_i, m_j, m_k) \tag{3.23}$$

$$I_{V_k}^{F_a}(m) = \frac{I_{F_b}^{V_k}(m)}{\sum_{m=0}^{M-1} I_{F_b}^{V_k}(m')} \tag{3.24}$$

where V_i, V_j, V_k are three Vector Nodes connected to the $n-th$ Factor Node and F_a and F_b are two Factor Nodes connected with $k-th$ Vector Node V_k. We calculate every $I_{F_n}^{V_i}(m_i)$ from Factor Node to Vector Node and $I_{V_k}^{F_a}(m)$ from Vector Node to Factor Node. Finally, after determined update number is finished symbol probability $Q_{V_k}(m)$ is calculated and decision made by

$$\hat{I}_k^{(u)} = \underset{m}{\operatorname{argmax}} \|Q_{V_k}(m)\| \tag{3.25}$$

where $Q_{V_k}(m) = I_{V_k}^{F_a}(m) I_{V_k}^{F_b}(m)$, and $\hat{I}_k^{(u)}$ is decoding output of factor graph for k'th symbol of user u.

3.3 A Novel Iterative SCMA Decoder with Bi-directional Decision Feedback (BDF) for MIMO System in Frequency Selective Channel

In this thesis, a novel receiver architecture is designed to improve system performance especially in multi-tap channel scenarios. Because, sparsity is destructed in multi-tap channel so the performance of the factor graph based receiver algorithm is decreased dramatically. Firstly MIMO is integrated into the system with N receiver antenna in the receiver part. In MIMO architecture received signal $\mathbf{r}[n]$ can be represented as:

$$\mathbf{r}[n] = \sum_{u=1}^{K} \mathbf{h}_u[n] * x_u[n] + \mathbf{n}[n] \tag{3.26}$$

As opposed to the conventional SCMA decoder, received signal is passed through a channel match filter for each user in receiver before processed in factor graphs. Integration of the MIMO in to the design caused to decrease in the effect of the ISI and ICI in the system which are caused by multi-tap channel because the diversity of channels of the users has increased. Thus, in the output of the match filter, transmitted signals from the entire user except the corresponding user for that channel match filter. And the side coefficients of cross match filter output for this corresponding user became weaker than center tap. The output of each match filter which is defined as y_u is processed in parallel factor graph blocks in which for each user corresponding match filter output is processed in the factor graph allocated for this user.

$$y_m[n] = \mathbf{h}_m^H[-n] * \mathbf{r}[n] = \sum_{l=0}^{L-1} \mathbf{h}_m^H[l]\mathbf{r}[n+l] \tag{3.27}$$

where $\mathbf{h}_m^H[n]$ is the channel match filter of user m.

Therefore, each user's estimation is made based on the factor graph which uses corresponding user's channel match filter as described in section 2.3.3.

One of the main differences between the operation of conventional SCMA decoder and Novel SCMA Decoder proposed in this thesis is the calculation of norm distance between possible transmitted signal and received signals in the output of the channel match filter block. In multi-tap scenario $\tilde{y}_m$ should be used instead of $\mathbf{r}$ in the input of factor graphs. In the first update of novel receiver, $\tilde{y}_m$ is calculated in that way: from y_m which is the channel match filter output of received signal, possible interferences

caused by multi-tap channel are substructed which are inter-symbol interference (ISI) caused by neighbor symbols and inter-chip interference (ICI) caused by the other chips of same symbol. Possible interferences are calculated by assuming that symbols which are decoding outputs of SC-FDE are transmitted from each user. Therefore predictions of SC-FDE are utilized and even if these predictions are not perfect, it gives good information about possible ISI and ICI. Therefore after elimination of these interferences factor graph has a better input signal to decode closer to the ideal case and performance of the factor graph is improved. Especially when the SC-FDE estimations are close to the real input symbols which occurs in high SNR, interference cancellation become better so system performance increases.

Therefore, $\tilde{y}_m$ which is the interference cancelled form of received signal according to current decoding outputs can be written as:

$$\begin{aligned}\tilde{y}_m\left[N_c k+i\right] = y_m\left[N_c k+i\right] &- \sum_{\substack{k'=0 \\ k'\neq k}}^{T-1} \sum_{u=1}^{K} \sum_{l=-L+1}^{L-1} p_{(m,u)}[l]\ \mathbf{c}^{(u)}_{\hat{I}^{(u)}_{k'}}[kN_c - k'N_c + i - l] \\ &- \sum_{u=1}^{K} \sum_{\substack{l=-L+1 \\ l\neq 0}}^{L-1} p_{(m,u)}[l]\ \mathbf{c}^{(u)}_{\hat{I}^{u}_{k}}[i-l] \end{aligned} \tag{3.28}$$

where $p^{(m,u)}[n] = h^H_m[n] * h_u[-n]$ is the cross channel response between the users u and m. $y_m\left[n\right]$ is output signal of channel match filter of user m which will be used in the decoding procedure of user m in factor graph. T is total number of symbol for a user and $\hat{I}^u_k\ \epsilon\ [1,2,3,...,M]$ is output of SC-FDE for k^{th} NOMA symbol of user u and $\mathbf{c}^u_{\hat{I}^u_t}[n]$ is predicted the transmitted codeword from user u in n^{th} chip according to the SC-FDE symbol estimations $\hat{I}^u_t$. Therefore, input of the m^{th} user's factor graph for k^{th} symbol can be expressed as:

$$\mathbf{z}^{(m)}_k = [\tilde{y}_m[kN_c+1] \quad \tilde{y}_m[kN_c+1] \quad ... \quad \tilde{y}_m[kN_c+N_c-1]]^T \tag{3.29}$$

Normally, in simple single tap scenario, in a given time slot received signal composes of only three active users' transmitted signal which are decided according to factor graph and noise. However in multi-tap scenario, not only active three users' messages

but also other users' messages received because of the interferences due to multipath. After calculating $\tilde{y}_m$ in order to calculate norm distance, the system model is assumed similar to simple model as conventional SCMA decoder in order to maintain the low decoder complexity. This means that channels are assumed to be perfect and thus, it is assumed that there is no ISI and ICI in the received signal. Perfect channel coefficients are calculated as, $p_{(u,m)}[n] = p_{(u,m)}[0]\delta_n$, so expected received signal can be simple expressed as:

$$y'_m[n] = \sum_{u=1}^{K} p_{(m,u)}[0]x_u[n] + n[n] \tag{3.30}$$

which is similar to form given in the literature. Therefore, expected input of the m^{th} user's factor graph for k^{th} symbol can be expressed as:

$$\tilde{\mathbf{z}}_k^{(m)} = [y'_m[kN_c+1] \quad y'_m[kN_c+1] \quad ... \quad y'_m[kN_c+N_c-1]]^T \tag{3.31}$$

So Norm distance can be calculated similar to simple SCMA decoder as:

$$\begin{aligned} d_k^w\left(I_i, I_j, I_l\right) &= -\frac{\|z_k^{(m)}[w] - S_1 - S_2 - S_3\|^2}{N_0} \\ S_1 &= p_{(m,i)}[0]c_{I_i}^{(i)}[w] \\ S_2 &= p_{(m,j)}[0]c_{I_j}^{(j)}[w] \\ S_3 &= p_{(m,l)}[0]c_{I_l}^{(l)}[w] \end{aligned} \tag{3.32}$$

where S_1, S_2, S_3 are possible transmitted signals from active three users during n^{th} time slot with perfect cross channel where $p_{(u1,u2)}$ and $c_{I_i}^{(i)}$ is the transmitted signal from user i for symbol I_i during corresponding time slot. After that $I_{F_n}^{V_i}$ and $I_{V_k}^{F_a}$ which are factor nodes and vector nodes of the massage passing algorithm in the factor graph are updated same as conventional SCMA decoder. Finally in the output of each factor graph symbol predictions are made for related user as:

$$\hat{I}_k^{(u)} = \underset{m}{\operatorname{argmax}} \|Q_{V_k}(m)\| \tag{3.33}$$

where $Q_{V_k}(m) = I_{V_k}^{F_a}(m)I_{V_k}^{F_b}(m)$ and $\hat{I}_k^{(u)}$ is decoding output of factor graph for k'th symbol of user u. In this way naturally predictions for every user are generated however only the predictions of the user whose channel match filter is used in the input of

the factor graph are taken into consideration and the estimations of other users are discarded. Therefore final predictions are acquired by combining corresponding user's predictions from each K parallel factor graph block. In addition, after first predictions are made in factor graph, according to these predictions an iterative feedback system is designed. So according to predicted symbols from factor graphs, possible ISI and ICI symbols are recalculated instead of SC-FDE equalizer outputs and they are subtracted from received signal in next iteration and parallel factor graph architecture is processed again. Therefore, it is expected that a better predictions than SC-FDE is acquired to cancel possible interferences.

$$\tilde{y}_m\left[N_c k+i\right] = y_m\left[N_c k+i\right] - \sum_{\substack{k'=0 \\ k'\neq k}}^{T-1} \sum_{u=1}^{K} \sum_{l=-L+1}^{L-1} p_{(m,u)}[l]\ \mathbf{c}^{(u)}_{\hat{I}^{(u)}_{k'}}[kN_c - k'N_c + i - l] - \sum_{u=1}^{K} \sum_{\substack{l=-L+1 \\ l\neq 0}}^{L-1} p_{(m,u)}[l]\ \mathbf{c}^{(u)}_{\hat{I}^{u}_{k}}[i-l] \tag{3.34}$$

where $p_{(u,m)}[n] = h_u^H[n] * h_m[-n]$ is cross channel match filter output of user u and user m, $y_m\left[n\right]$ is output signal of channel match filter of user m. T is total number of symbol for a user and $\hat{I}^u_k\ \epsilon\ [1,2,3,...,M]$ is output of u^{th} user's factor graph for k^{th} NOMA symbol and $\mathbf{c}^u_{\hat{I}^u_t}$ is the expected transmitted codeword from user u in k^{th} SCMA symbol according to the symbol estimation $\hat{I}^u_t$ from factor graph.

This iterative decision feedback mechanism continuies for a certain number of iterations. System model of novel receiver architecture can be seen from Figure 3.3 .

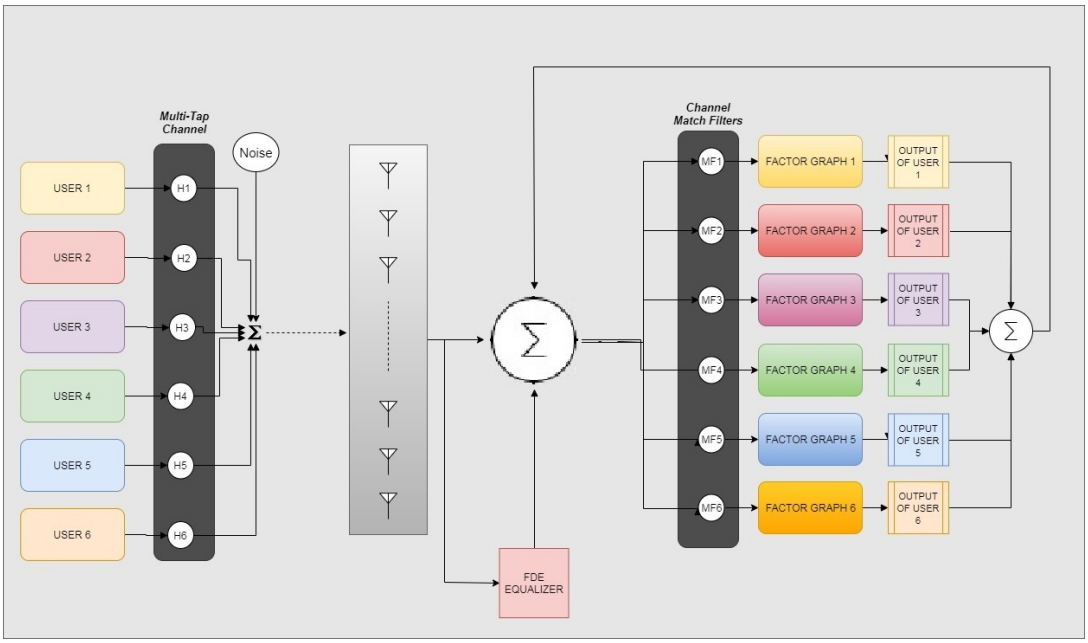

Figure 3.3: Novel MIMO RECEIVER DIAGRAM

CHAPTER 4

PERFORMANCE ANALYSIS BASED ON ACHIEVABLE INFORMATION RATE(AIR)

4.1 Mismatched Decoding Capacity via Generalized Mutual Information

In order to make performance analysis of designed novel receiver architectures only providing "Bit Error Rates" (BER) comparisons is not adequate. Therefore, as a part of this thesis, in order to support our work and provide a better comparison between different scenarios, a capacity comparison is made which is called as "Achievable Information Rate" (AIR). AIR is a quantity which corresponds to the reliable information rate that can be transmitted through a given channel. For a system with a uniform input symbol alphabet AIR can be expressed as [23]:

$$AIR = \log_2 |A_X| - E_{X,Y} \left\{ \log_2 \left(\frac{\sum_{x' \in A_x} \hat{p}\left(Y|x'\right)}{\hat{p}\left(Y|X\right)} \right) \right\} \tag{4.1}$$

where $|A_X|$ is the alphabet size of codebook, $\hat{p}\left(Y|x', h\right)$ is the approximate probability density function of signal Y is received when the symbol x' is transmitted and X is the real transmitted signal from corresponding user. In order to get fair AIR value, calculated value should be divided by the number of resource elements which is number of time chips for a single SCMA symbol. Typically, capacity parameter originally calculated from exact values of the probabilities of the received signal given transmitted symbol. However in SC-SCMA there is interference so it is not possible to obtain exact probability density function values. So instead of exact values of probability density function, probability density function which are close to the exact values of density functions are utilized and this approach is referred as mismatched decoding [24]. Because of the fact that calculation of $\hat{p}\left(Y|x'\right)$ is not simple, equation can be

rewritten by using bayes rule which states that:

$$\hat{p}\left(Y|x'\right) = \hat{p}\left(x'|Y\right)\frac{\hat{p}\left(Y\right)}{\hat{p}\left(x'\right)} \tag{4.2}$$

So our equation can be expressed as:

$$AIR = \log_2\left|A_X\right| - E_{X,Y}\left\{\log_2\left(\frac{\sum_{x'\in A_x}\hat{p}\left(x'|Y\right)\frac{\hat{p}(Y)}{\hat{p}(x')}}{\hat{p}\left(X|Y\right)\frac{\hat{p}(Y)}{\hat{p}(X)}}\right)\right\} \tag{4.3}$$

As indicated before in SC-SCMA, codewords are equally likely so $\hat{p}\left(X\right)$ and $\hat{p}\left(x'\right)$ are equal to $\frac{1}{|A_X|}$.So we can calculate AIR parameter from approximately probability density functions as:

$$AIR = \log_2\left|A_X\right| - E_{X,Y}\left\{\log_2\left(\frac{\sum_{x'\in A_x}\hat{p}\left(x'|Y\right)}{\hat{p}\left(X|Y\right)}\right)\right\} \tag{4.4}$$

4.2 Air Analysis of Proposed Architectures

AIR depends on the total number of constellation points of transmitted signal and $\hat{p}\left(x|Y\right)$ as it can be seen in equation (4.4) because $|A_X|$ is a constant value and $\sum_{x\in A_x}\hat{p}\left(x|Y\right)$ equal to the 1. In order to calculate the AIR parameter in different scenarios studied in this thesis, calculation of the probability of transmitted symbol from received signal is necessary and this value calculated differently in each scenario because the symbol estimations are done with different decision criteria.

4.2.1 Single User ML Decoding

In Single User ML Decoding received signal is passed through the corresponding channel match filter for every user and each user's estimations are done by using ML Estimate which compares symbol-wise norm distances between received signal's corresponding indexes and possible transmitted signal as described at equation (3.6). The probability function for normal distribution is:

$$P\left(x\right) = \frac{1}{\sigma\sqrt{2\pi}}e^{-\frac{(x-\mu)^2}{2\sigma^2}} \tag{4.5}$$

where σ^2 is variance and μ is the mean. Therefore we can say that $\hat{P}(x|Y,h) \approx e^{-d^2/N_0}$ where d is the norm distance calculated in ML estimator.

4.2.2 Single User ML Decoding with SC-FDE

Similar to Single User ML Decoding case, in SC-FDE scenario estimations of the users' transmitted symbols are done with ML estimator which consider the norm difference between equalizer output corresponds to the relevant user's corresponding symbol and possible transmitted codebooks of the same user. Therefore, this norm difference can be utilized directly to get $\hat{p}(x|Y)$ such that, $\hat{p}(x|Y) \approx e^{-d^2}$ where d is the norm distance calculated in ML estimator.

4.2.3 SC-SCMA Decoder

In SC-SCMA decisions over the transmitted signals are done over the $Q_{V_k}(x) = I_{V_k}^{F_a}(x) I_{V_k}^{F_b}(x)$ where F_a, F_b are two variable node connected to user k in the factor graph and $I_{V_k}^{F_a}(x)$ and $I_{V_k}^{F_b}(m)$ are iteratively computed in the factor graph over I_f^v values, m corresponds to the possible constellation point. In factor graph $Q_{V_k}(x)$ values can be calculated from $\hat{P}(x|Y)$ where $\hat{P}(x|Y) \approx Q_{V_k}(x)$.

CHAPTER 5

SIMULATION RESULTS

In this chapter, simulation results are presented for different structures with different parameters. Simulation results mainly show the Bit Error Rate (BER) and Achievable Information Rate (AIR) of different structures with different system parameters under different $\frac{Eb}{N_0}$ values. In this thesis, a SCMA network model with six users and four resource elements is studied. The main variable system parameters in this study are following:

- Number of total constellation points per single SCMA symbol (bits per symbol)
- Number of total and active taps in channel
- Number of receiver Antenna in Receiver
- Angle of spread of the delay taps

Also in order to show support of the MIMO in receiver structure, simulation results for cross channel match filter outputs are provided. In graphs 5 different plots can be seen; firstly performance of the direct ML estimation, secondly performance of the direct iterative factor graph performances, thirdly performance of SC-FDE and fourthly, performance of the iterative factor graph which utilize the SC-FDE outputs anf finally the performance of the system unde perfect interference cancellation. Mainly, in simulations four different scenarios are analyzed.

5.1 Single Tap Channel with Single Receiver Antenna Scenario

Firstly, performance of conventional SCMA decoder is simulated. In this scenario, channel is assumed as single-tap channel and in receiver only one receiver antenna is occupied. Therefore, in this model there is no ISI or ICI which cause destruction in the sparsity of the SCMA codewords. For this reason without using any novel receiver architecture, system can decode received symbols in factor graph with a high performance. In this model two different channel models are used; first a AWGN channel is used in which all the channel coefficients are assumed to be 1, second a Rayleigh channel between transmitter and receiver. Corresponding simulation results can be seen in figure 5.1 and figure 5.2 respectively. In this scenario bi-directional iterative decision feedback mechanism is not used because it is used to reduce interferences. Also AIR graph of this schemes are provided for these two models in figure 5.3 respectively.

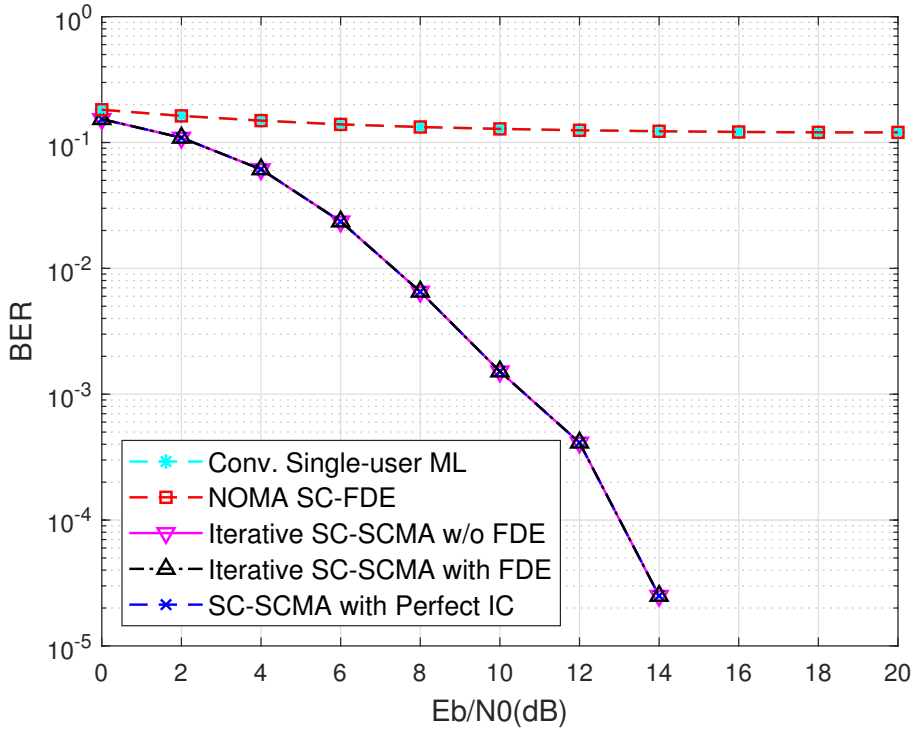

Figure 5.1: BER vs E_b/N_0 Performance in Single Tap AWGN Channel

Simulation results indicate that, BER performance is reduced in Rayleigh channel because in addition to noise, non-uniform channel causes a decrease in the performance

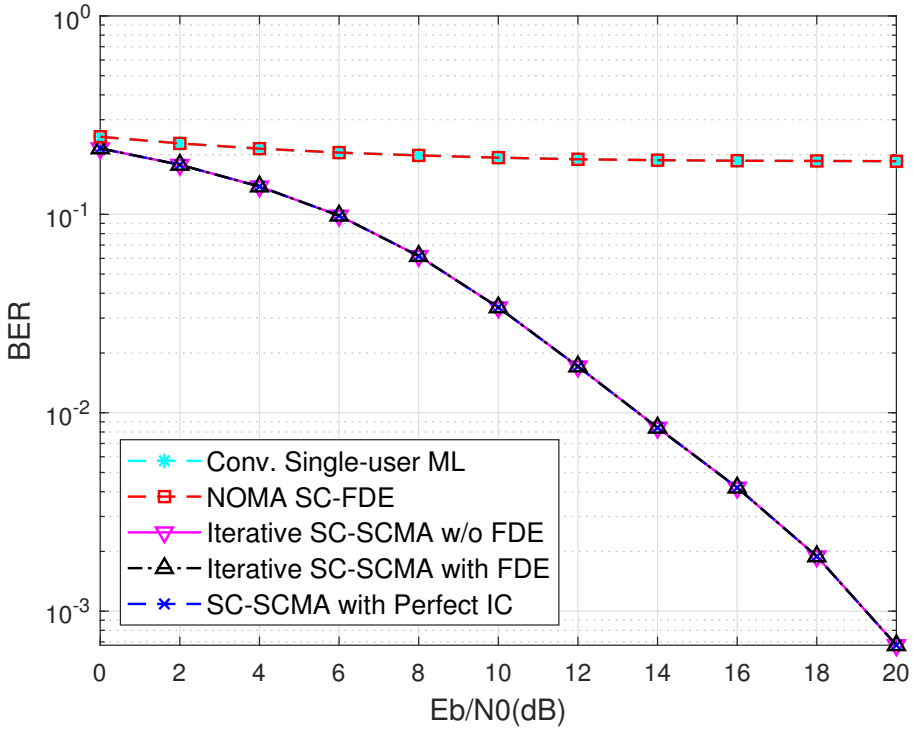

Figure 5.2: BER vs E_b/N_0 Performance in Single Tap Rayleigh Channel

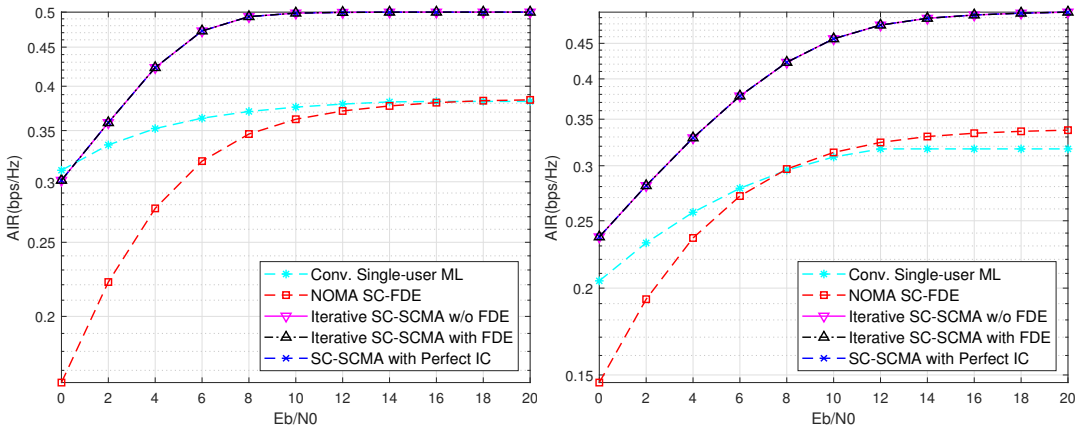

(a) Single Tap AWGN Channel

(b) Single Tap Rayleigh Channel

Figure 5.3: AIR vs E_b/N_0 Performance in Single Tap Channels

of the factor graph when it is compared with AWGN channel. However, both schemes give good BER performances for a communication network. Also because of the fact that there is no ISI and ICI, performance of the iterations of factor graph is same with perfect interference cancellation case. Also SC-FDE doesnot works.

5.2 Multi Tap Channel with Single Receiver Antenna Scenario

Secondly, a multipath channel with 16 taps with 6 active taps instead of single tap channel scenario is simulated in order to show the dramatic performance decrease in conventional receiver architectures. Simulation results for BER performance and AIR graphs can be seen at figure 5.4 and figure 5.5.

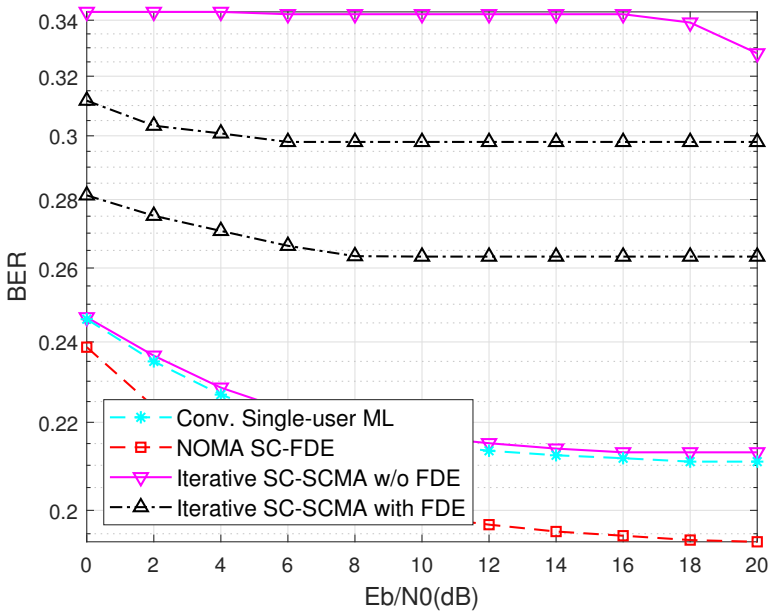

Figure 5.4: BER vs E_b/N_0 Performance with Single Receiver Antenna, 16 Taps, 6 Active Taps Channel

As it can be seen from the simulation results, system is destructed and even in high E_b/N_0 values system cannot decode received signal. Main reason for this problem is that effect of ISI and ICI is dramatic so sparsity of the SCMA codewords is destructed and sparsity cannot recovered in the receiver. Thus, the performance of the system decreased dramatically when it is compared with the performance of the single tap channel. In this model bi-directional iterative decision feedback mechanism with group of factor graphs is utilized, however because of the fact that estimations of SC-FDE and factor graphs are not good, performance of the system decreased in next iterations because interference cancellations are done based on the false estimations and received signal worsen. Thus, it can be deduced that novel receiver architecture is necessary to overcome this problem.

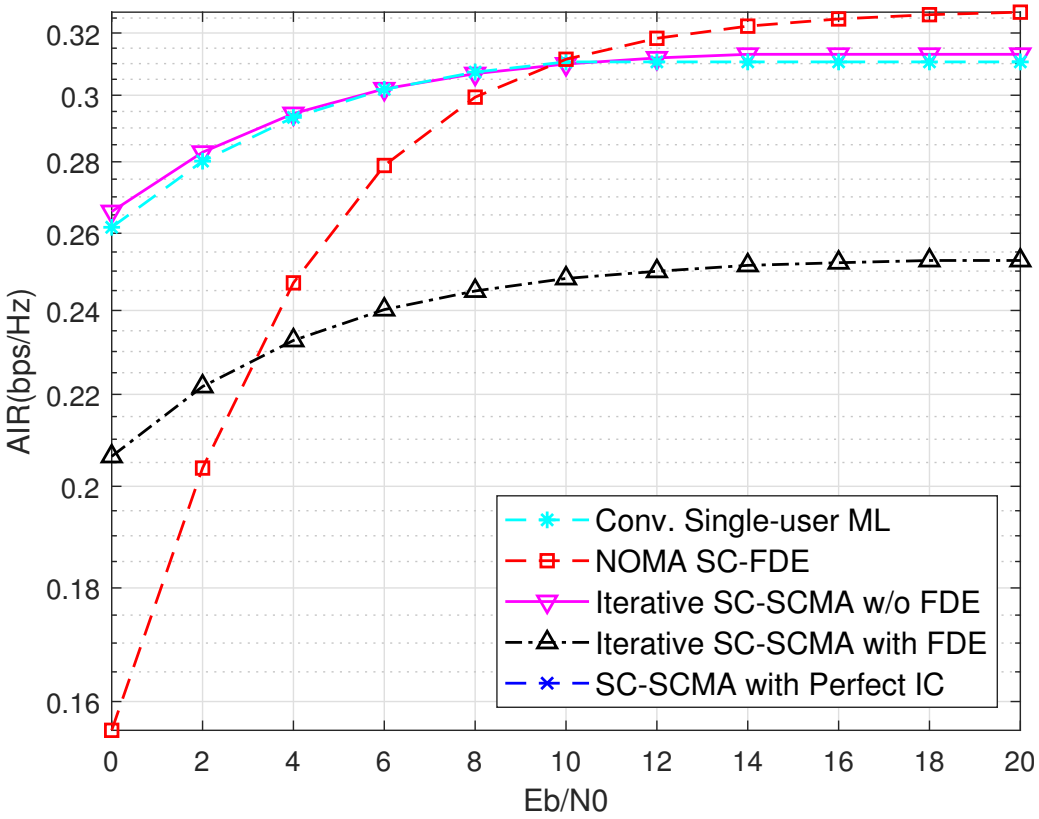

Figure 5.5: AIR vs E_b/N_0 Performance with Single Receiver Antenna, 16 Taps with 6 Active Taps Channel

5.3 Single Tap Channel with Multiple Receiver Antenna Scenario

Thirdly, MIMO is integrated in the conventional SCMA architecture in single tap channel. Results of the Rayleigh channel with multiple receiver antenna can be seen in figure 5.6 and AIR performance for corresponding scenario can be seen in figure 5.7.

When the results of figure 5.6 and figure 5.2 compared it can be interpreted that using multiple receiver antenna and processing received signals together improves the performance of receiver in single tap channel scenario.

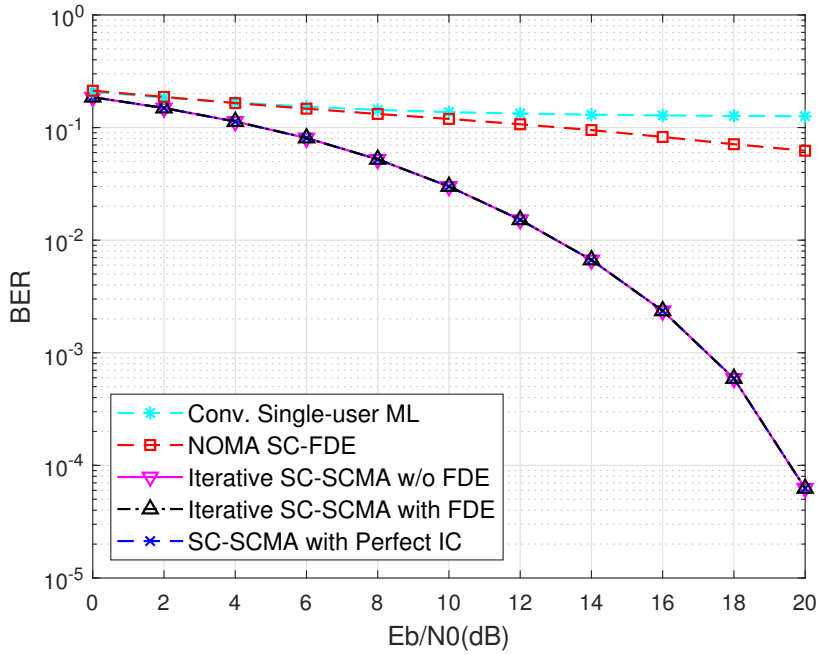

Figure 5.6: BER vs E_b/N_0 Performance with 10 Receiver Antenna, Single Tap Channel

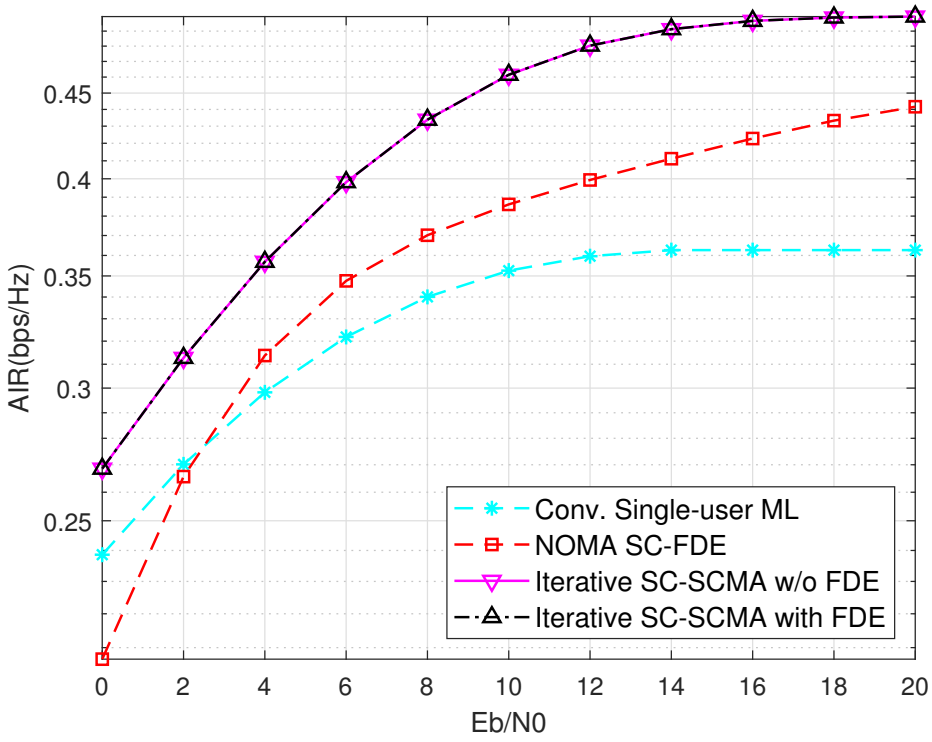

Figure 5.7: AIR Performance with 10 Receiver Antenna, Single Tap Channel

5.4 Multi Tap Channel with Multiple Receiver Antenna Scenario

Fourthly, the performance of the novel receiver architecture which utilizes multiple receiver antennas (MIMO) under multi-tap channel is analyzed. In this scenario there are several factors, which affect the performance of the system and as stated before. Thus, the performance of the proposed structure is analyzed different system parameters. Firstly, in order to test the effect of the number of receiver antenna, system simulated with different number of antennas.

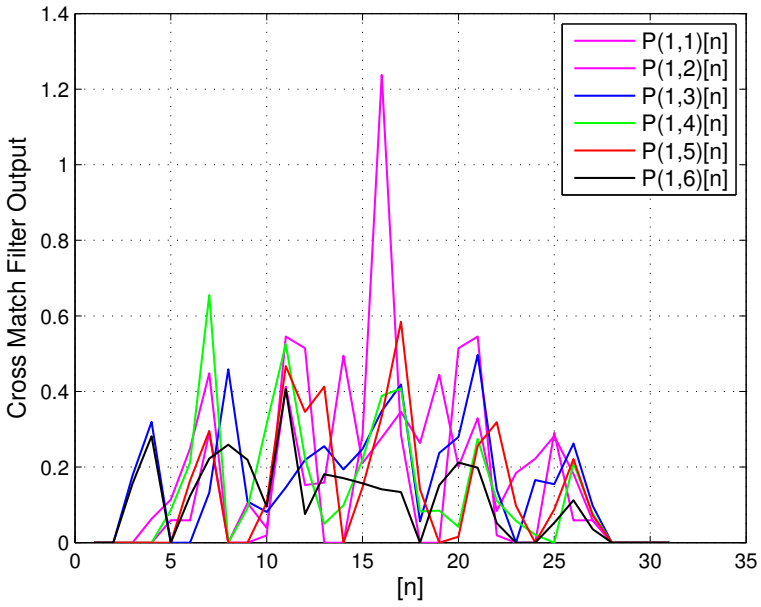

Figure 5.8: Cross Channel Match Filter Output of First User with Single Antenna

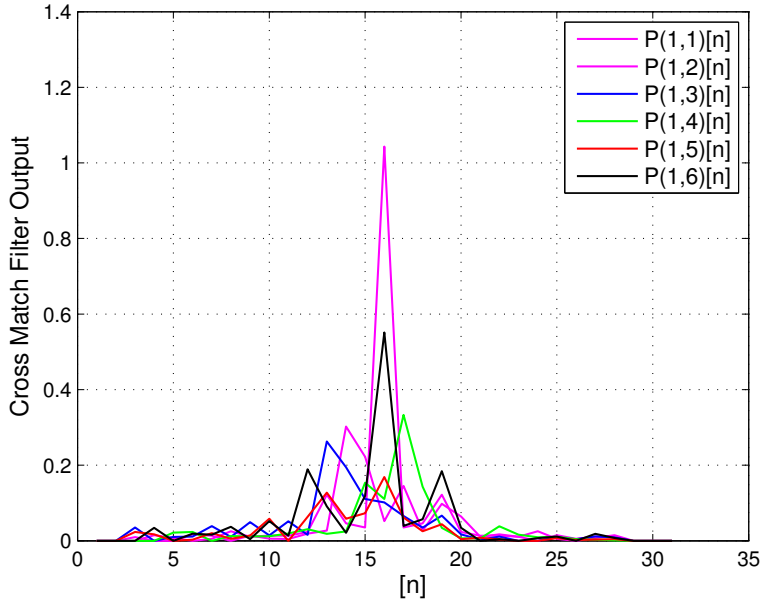

Figure 5.9: Cross Channel Match Filter Output of First User with Multiple Antenna

In MIMO architecture, multiple receiver antennas is utilized therefore output of the cross channel match filters between two different users and self-match filter output of a user become more distinct and center tap coefficient are more powerful than side taps as it can be seen from figure 5.8 and figure 5.9. Therefore, in match filter block, power of delay taps which causes interference and signal of other users are weakened, hereby this receiver architecture provides more legitimate estimates. Simulations are done for 4 constellation points and 16 constellation points separately. The simulation results for 4 constellation point with 3, 5, 10, 20 antennas can be seen at figure 5.10, figure 5.11, figure 5.12,figure 5.13 respectively and corresponding AIR results can be seen at figure 5.14. The simulation results for 16 constellation point with 5, 10, 20, 50 antennas can be seen at figure 5.15, figure 5.16, figure 5.17,figure 5.18 respectively and corresponding AIR results can be seen at figure 5.19.

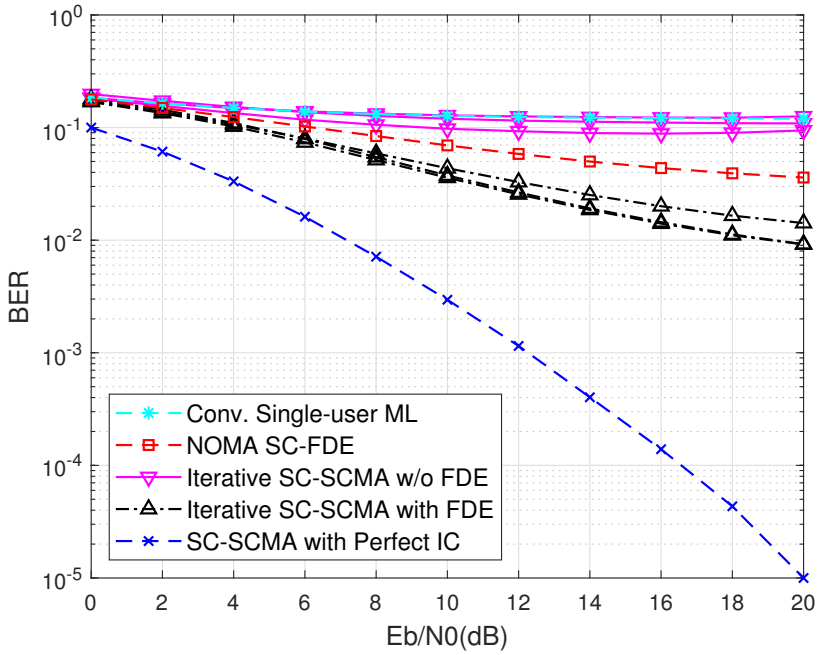

Figure 5.10: BER vs E_b/N_0 Performance with 3 Receiver Antenna, 16 Taps, 6 Active-taps, 10^o Angular Spread, 4 Constellation Points

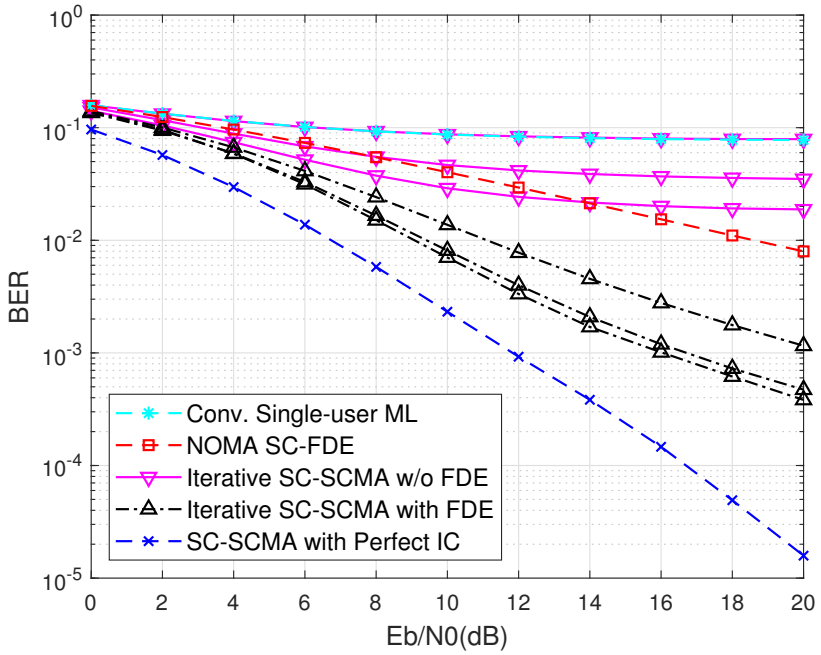

Figure 5.11: BER vs E_b/N_0 Performance with 5 Receiver Antenna, 16 Taps, 6 Active-taps, 10^o Angular Spread, 4 Constellation Points

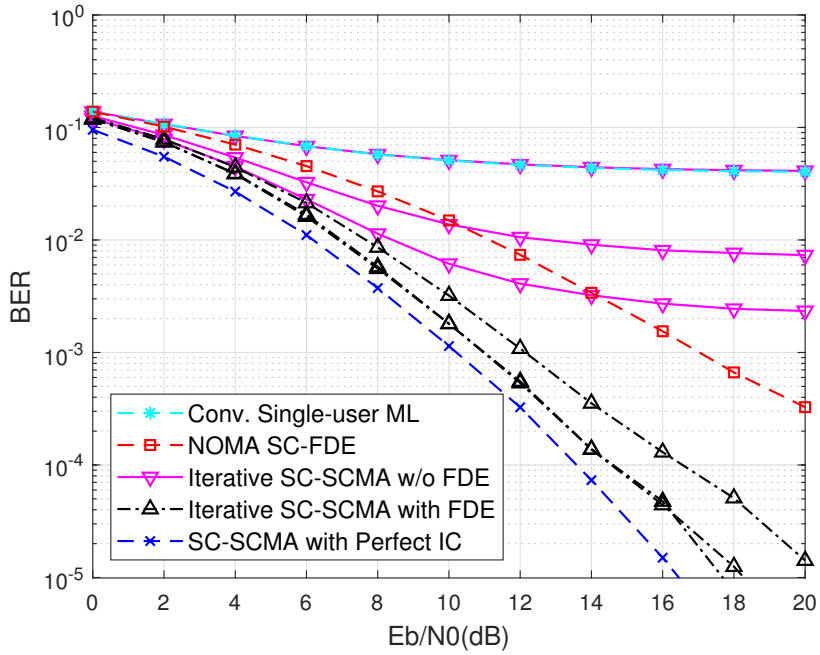

Figure 5.12: BER vs E_b/N_0 Performance with 10 Receiver Antenna, 16 Taps, 6 Active-taps, 10^o Angular Spread, 4 Constellation Points

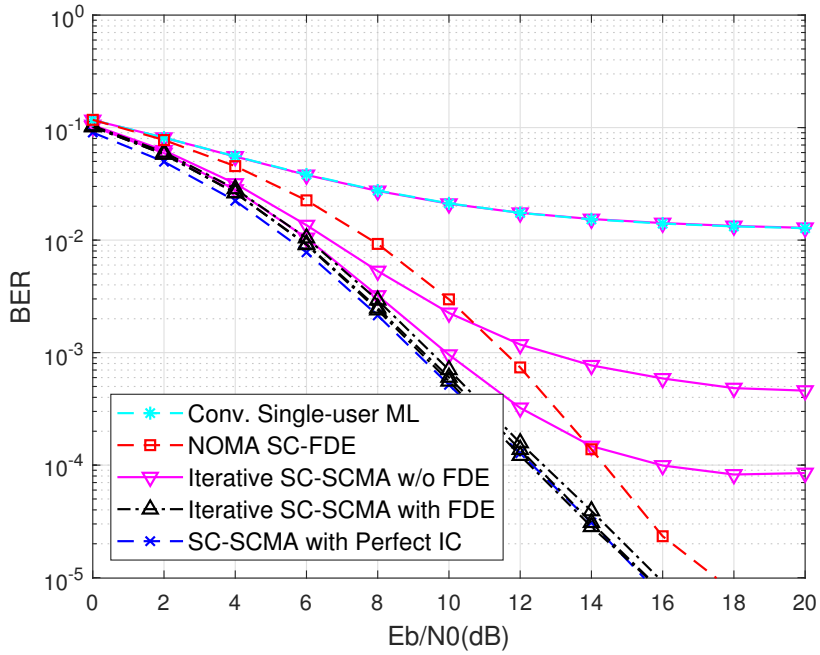

Figure 5.13: BER vs E_b/N_0 Performance with 20 Receiver Antenna, 16 Taps, 6 Active-taps, 10^o Angular Spread, 4 Constellation Points

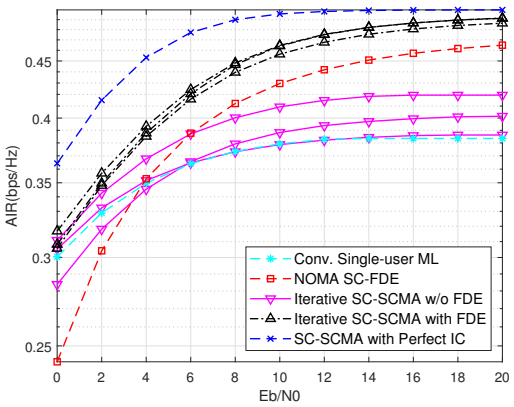

(a) 3 Receiver Antennas

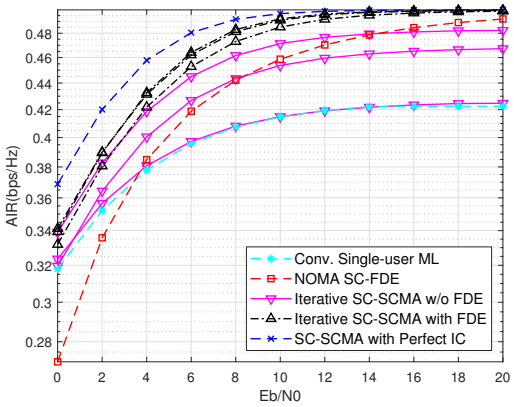

(b) 5 Receiver Antennas

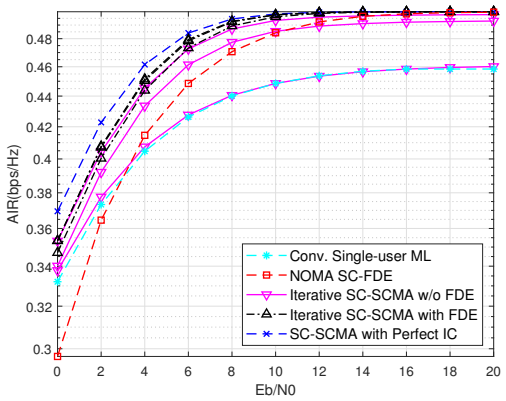

(c) 10 Receiver Antennas

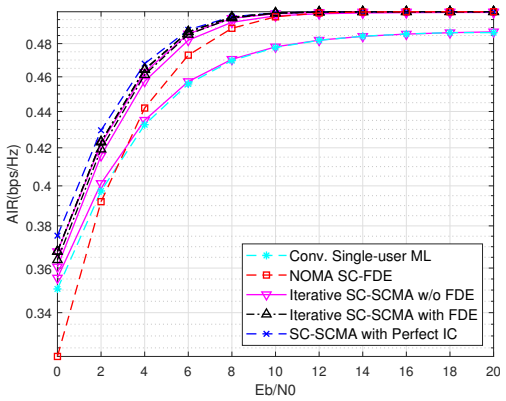

(d) 20 Receiver Antennas

Figure 5.14: AIR vs E_b/N_0 Performance with Different Number of Receiver Antenna, 16 Taps, 6 Active-taps, 10^o Angular Spread, 4 Constellation Points

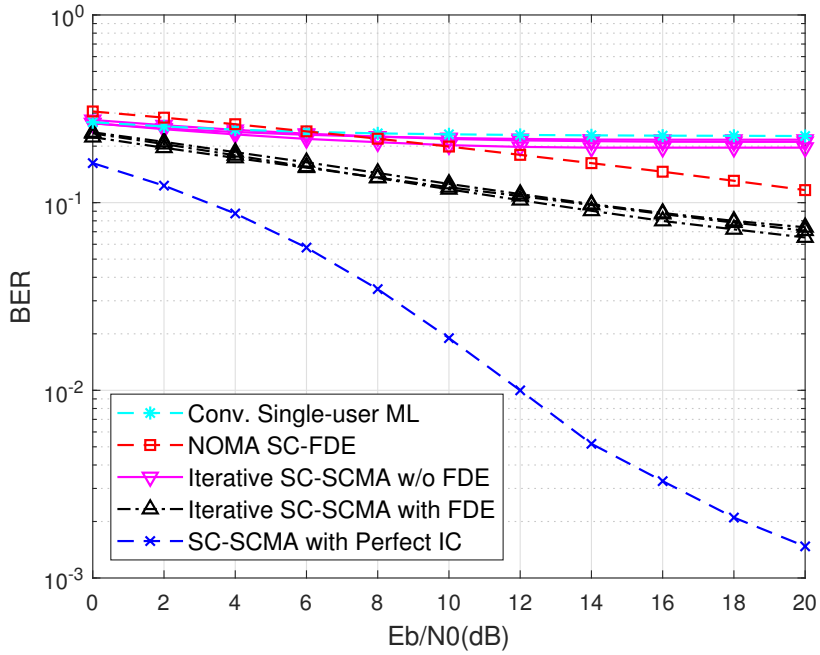

Figure 5.15: BER vs E_b/N_0 Performance with 5 Receiver Antenna, 16 Taps, 6 Active-taps, 10^o Angular Spread, 16 Constellation Points

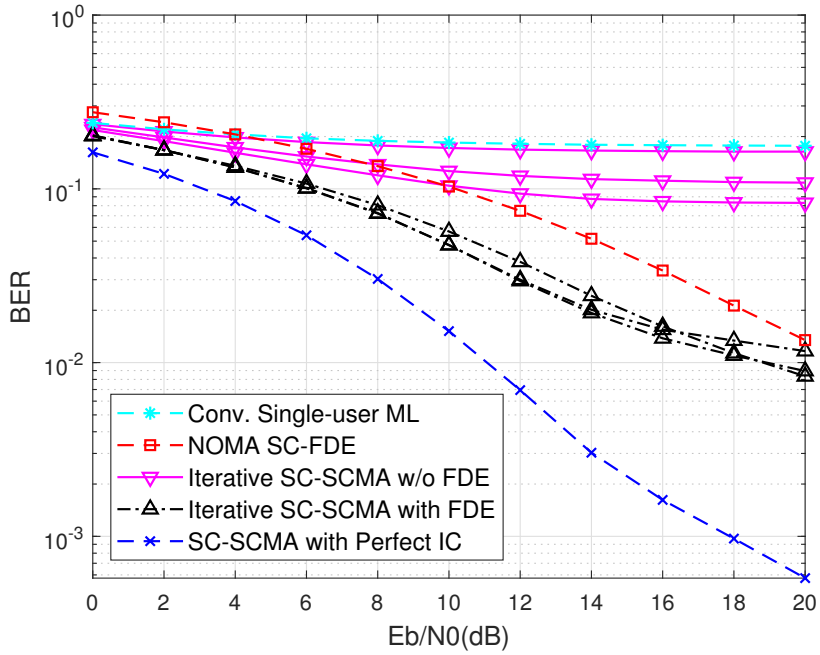

Figure 5.16: BER vs E_b/N_0 Performance with 10 Receiver Antenna, 16 Taps, 6 Active-taps, 10^o Angular Spread, 16 Constellation Points

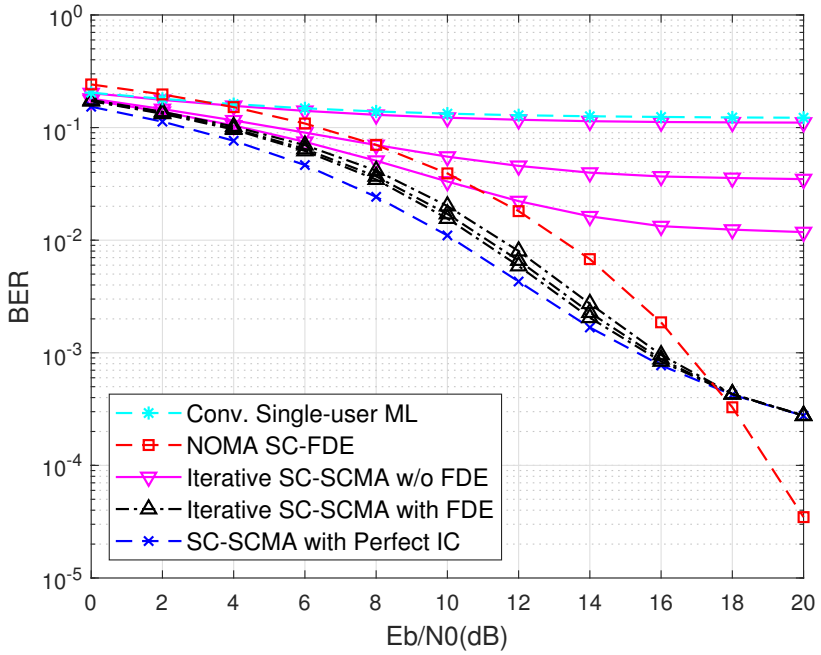

Figure 5.17: BER vs E_b/N_0 Performance with 20 Receiver Antenna, 16 Taps, 6 Active-taps, 10^o Angular Spread, 16 Constellation Points

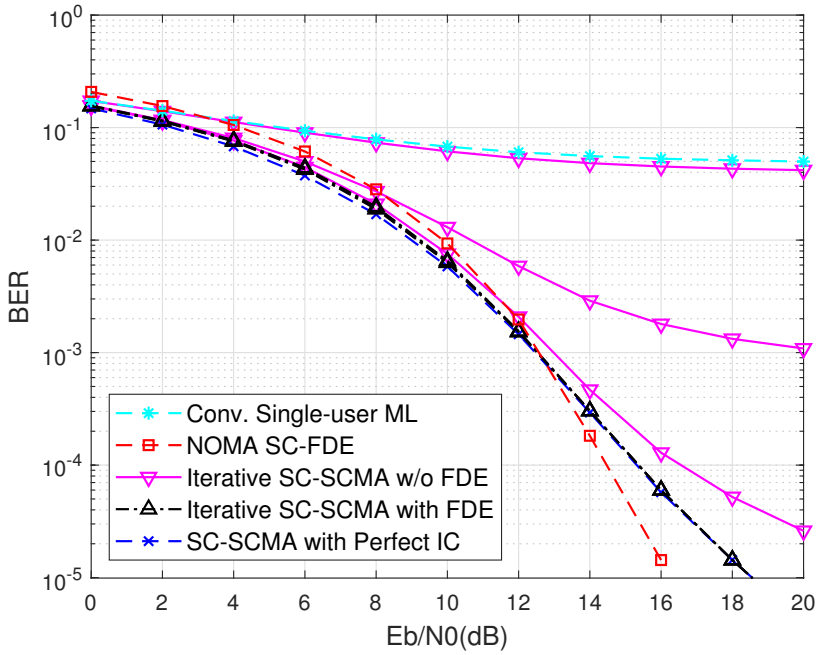

Figure 5.18: BER vs E_b/N_0 Performance with 50 Receiver Antenna, 16 Taps, 6 Active-taps, 10^o Angular Spread, 16 Constellation Points

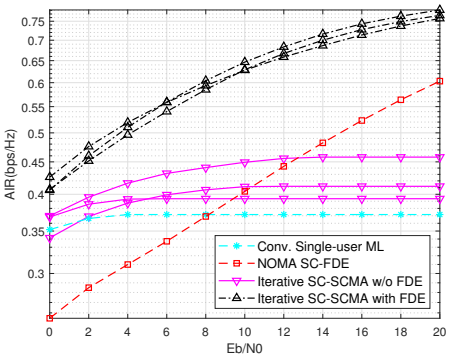

(a) 5 Receiver Antennas

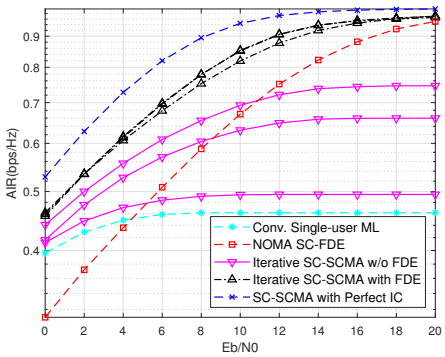

(b) 10 Receiver Antennas

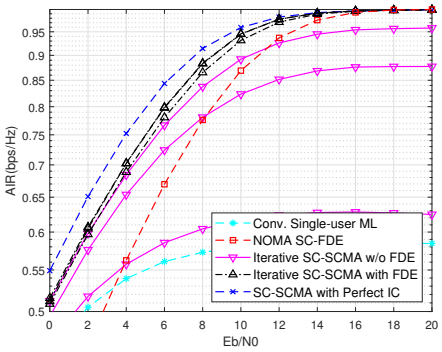

(c) 20 Receiver Antennas

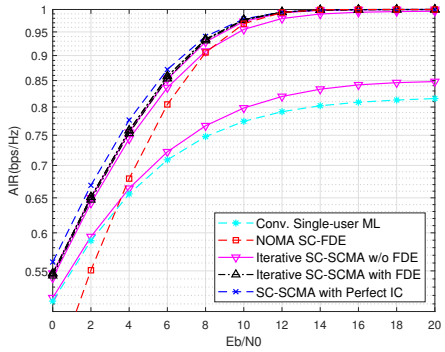

(d) 50 Receiver Antennas

Figure 5.19: AIR vs E_b/N_0 Performance with Different Number of Receiver Antenna, 16 Taps, 6 Active-taps, 10^o Angular Spread, 16 Constellation Points

Results indicate that, system performance is improved when the number of receiver antenna is increased. The effect of interferences is suppressed. Therefore, even in the first iteration good estimations are obtained. In next iterations, the system uses previous predictions similarly to previous case. According to these estimates, ISI and ICI are calculated and these parts are subtracted from the received signal. So in every iteration, system's BER result improves. Also SC-FDE provides good a-priori estimations for factor graph so performance of the bi-directional iterative feedback mechanism which uses output of SC-FDE outperforms direct factor graph estimations and the performance of the architecture approaches the performance of the system with perfect interference cancellation. In scenario with high SNR and high number of an-

tenna, direct SC-FDE can give better performance than factor graph as it can be seen from figure 5.17 and 5.18. Besides, in 4 constellation point scheme, system performance is high with more than 5 antennas, but in system in which 16 constellation points are utilized high performance is attained after 20 receiver antennas.

Secondly, effect of the channel parameters which are total and active tap numbers in the channel, in the performance of the system is analyzed. For that reason simulations are done with 16 taps with 16 active taps and 64 taps with 16 active taps when number of receiver antenna is 10 and angular support is taken as 10°. BER performance of the simulation for 16 taps with 16 active taps can be seen at figure 5.20 and corresponding AIR result can be seen at figure 5.21 and BER performance of the simulation for 64 taps with 16 active taps can be seen at figure 5.22 and corresponding AIR result can be seen at figure 5.23

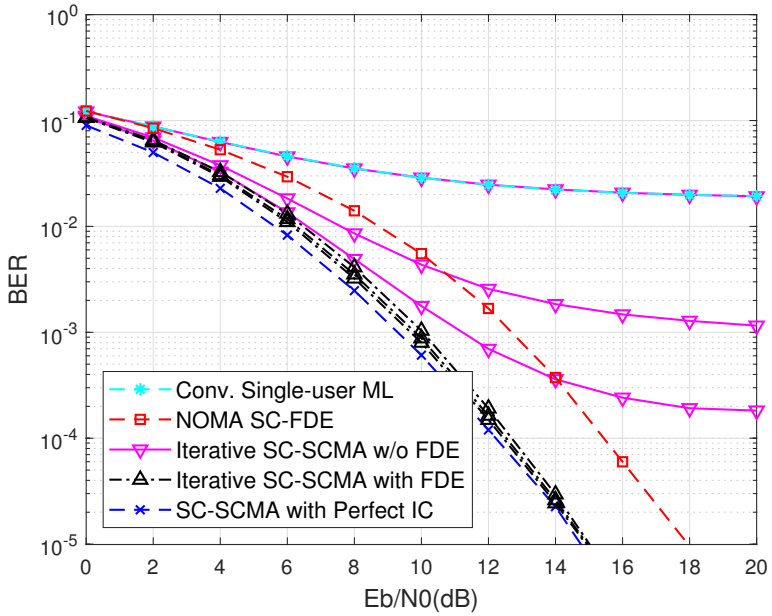

Figure 5.20: BER vs E_b/N_0 Performance with 10 Receiver Antenna, 16 Taps, 16 Active-taps, 10^o Angular Spread, 4 Constellation Points

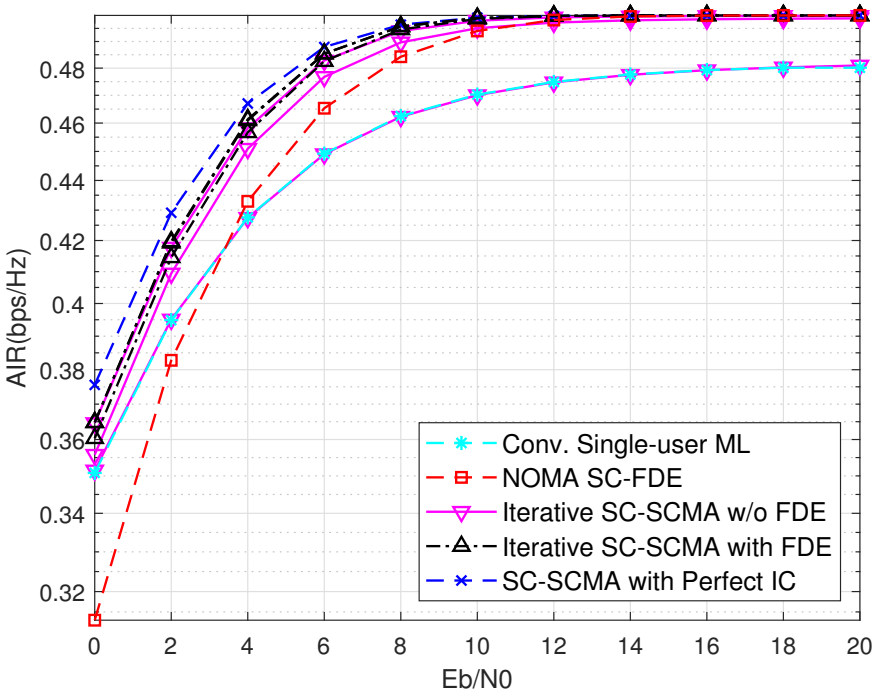

Figure 5.21: AIR vs E_b/N_0 Performance with 10 Receiver Antenna, 16 Taps, 16 Active-taps, 10^o Angular Spread, 4 Constellation Points

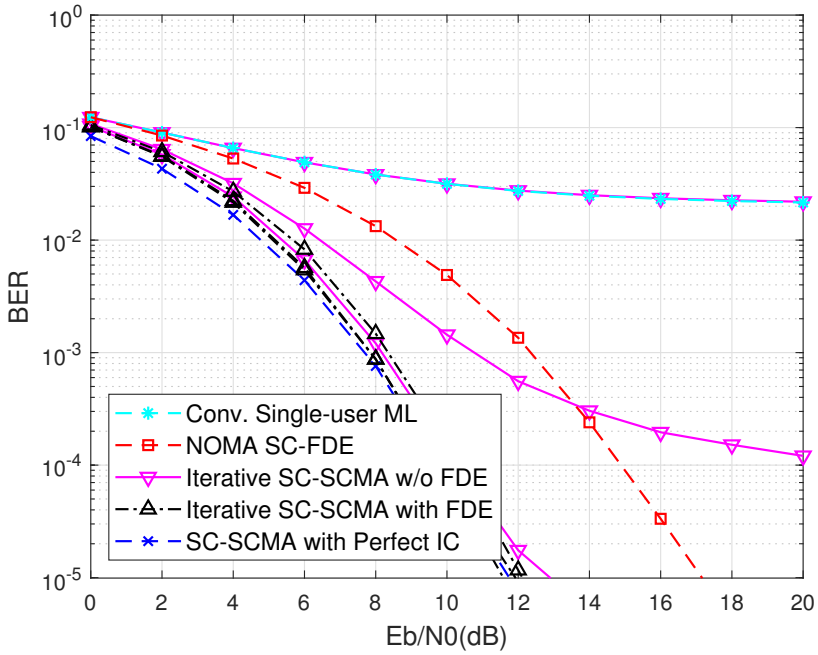

Figure 5.22: BER vs E_b/N_0 Performance with 10 Receiver Antenna, 64 Taps, 16 Active-taps, 10^o Angular Spread, 4 Constellation Points

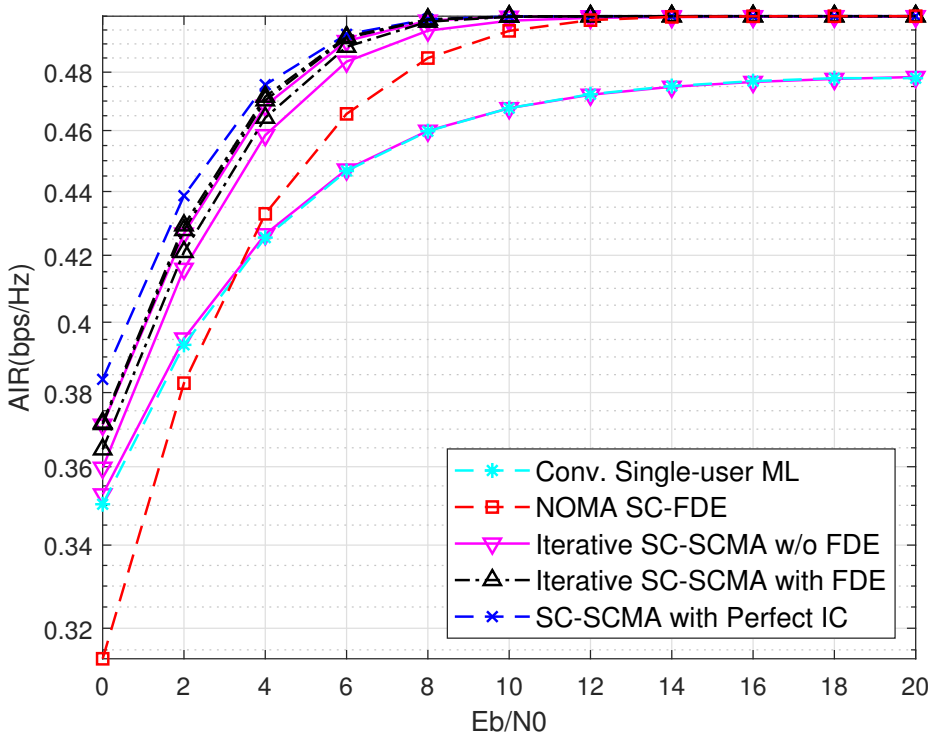

Figure 5.23: AIR vs E_b/N_0 Performance with 10 Receiver Antenna, 64 Taps, 16 Active-taps, 10^o Angular Spread, 4 Constellation Points

Results show that; when the number of active taps and number of total taps increased, performances of the schemes improves. Main reason behind this improvement is that when the number of total taps and active taps are increased cross channel match filter outputs become more distinct and effect of ISI and ICI decreases in the received signal.

Finally, performance of the novel receiver architecture with different angular support values is studied. In this simulations channel assumed as 16 taps with 6 random active taps and in receiver 10 receiver antenna is occupied and angular spread is assumed as 3° 10° 20° 45° so corresponding BER performances can be seen at figure 5.24, figure 5.12, figure 5.25, figure 5.26 and corresponding AIR performances are given at figure 5.27.

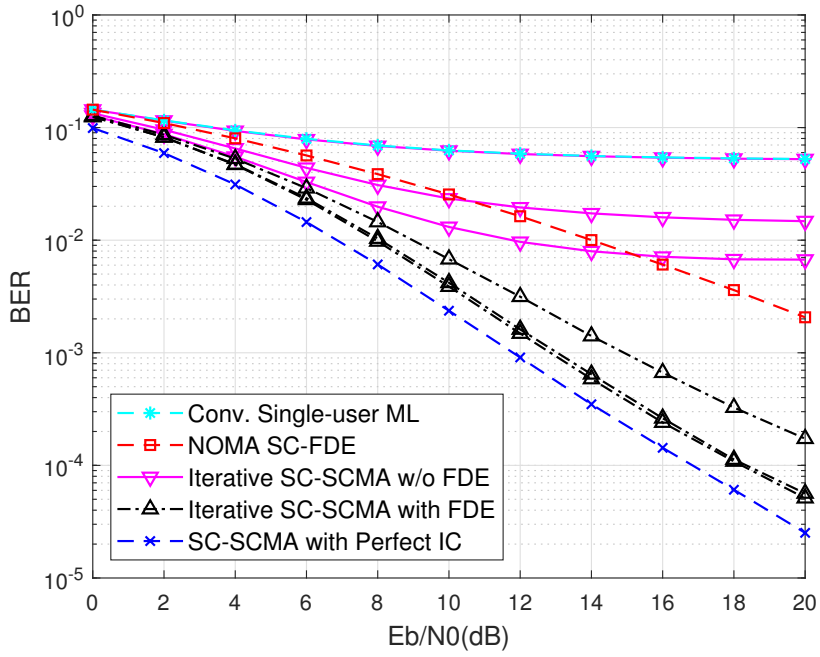

Figure 5.24: BER vs E_b/N_0 Performance with 10 Receiver Antenna, 16 Taps, 6 Active-taps, 3^o Angular Spread, 4 Constellation Points

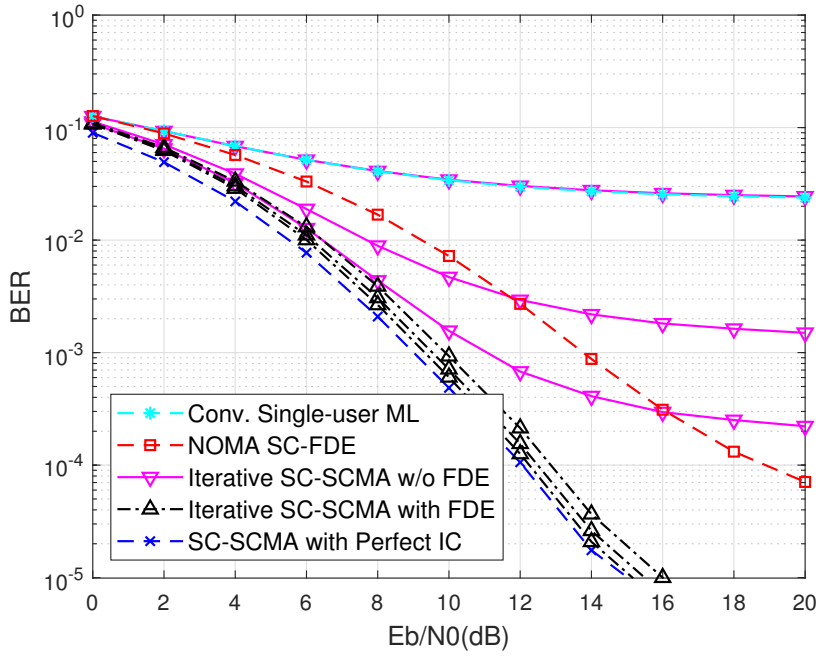

Figure 5.25: BER vs E_b/N_0 Performance with 10 Receiver Antenna, 16 Taps, 6 Active-taps, 20^o Angular Spread, 4 Constellation Points

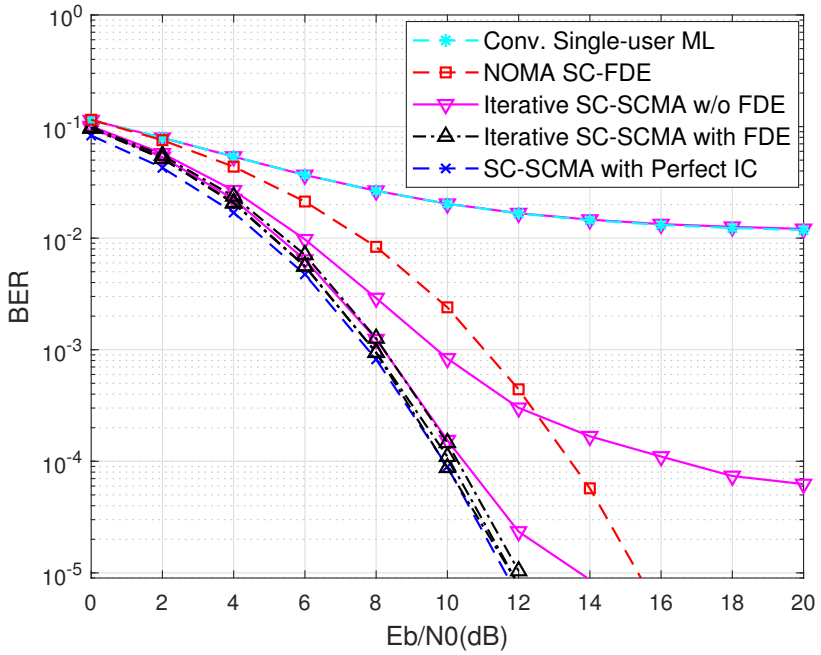

Figure 5.26: BER vs E_b/N_0 Performance with 10 Receiver Antenna, 16 Taps, 6 Active-taps, 45^o Angular Spread, 4 Constellation Points

Results show that; when the angular spread is increased, the correlations between the antenna elements are decreased therefore, the separation of the users in the antennas become more difficult. In ideal scenario with uncorrelated antennas the system performance will be best however, in real life scenarios antennas are always correlated so angular spread is a very important parameter which affects the BER performance.

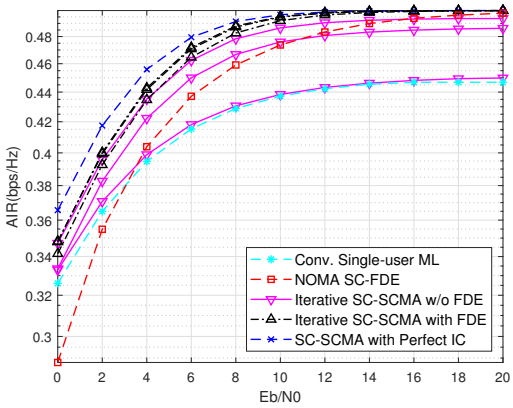

(a) 3^o Angular Spread

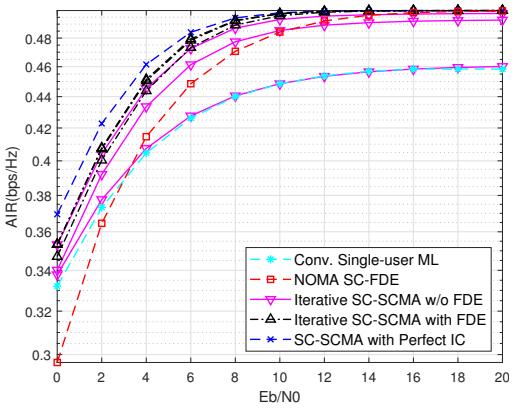

(b) 10^o Angular Spread

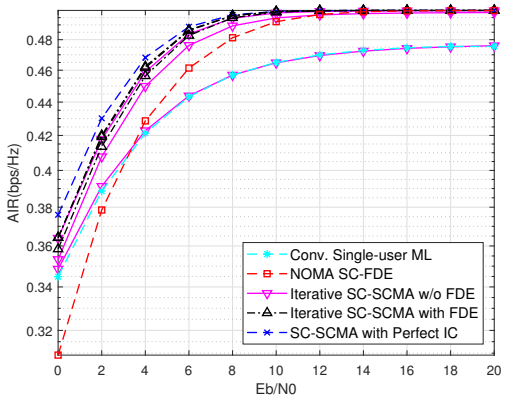

(c) 20^o Angular Spread

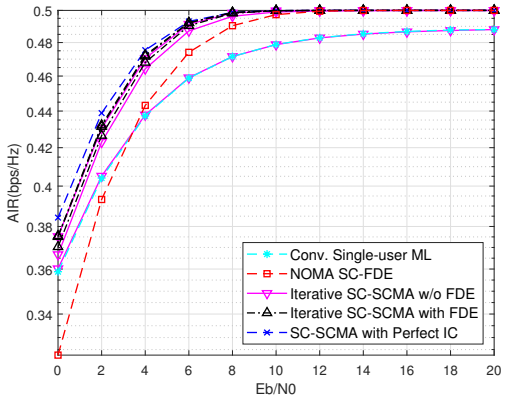

(d) 45^o Angular Spread

Figure 5.27: AIR vs E_b/N_0 Performance with Different Angular Spreads, 10 Receiver Antenna, 16 Taps, 6 Active-taps, 4 Constellation Points

CHAPTER 6

CONCLUSION

Conventional communication schemes are always designed over the idea of utilization of the orthogonal resources. However orthogonal resources are limited thus orthogonal communication schemes cannot address the requirements a great interest on Non-Orthogonal communication schemes are raised. In this thesis, in order to provide an alternative for next generation communication systems, a novel receiver model for single-carrier SCMA is proposed which is a NOMA technique. The performances of the proposed models are analyzed under different resource allocation, receiver architecture and channel models. Lots of researches concentrated on multi-carrier NOMA schemes to find an alternative solution for next generation network systems, despite of the fact that it brings lots of disadvantages. However, results of this study indicate that, single carrier SCMA modulation schemes with novel receiver architecture which consist of SC-FDE, MIMO receiver design and bi-directional iterative decision feedback model has a good performance even in frequency selective channels. In massive MIMO scenario receiver antennas can provide service for several NOMA groups simultaneously and each group consist of users with spatially correlated channels. Novel receiver architecture studies the performance of the single NOMA group. This novel receiver architecture mainly recover sparsity with the help of proposed bi-directional iterative feedback mechanism which cancels the interference according to predictions of equalizer and factor graph block. The performance of the system depends on several factors such as total constellation points, number of receiver antenna for MIMO design, total multi-tap and active tap number in the channel, angular spread of the multipath delays. Therefore, when the performance of the novel receiver architecture is taken into consideration, single carrier SCMA can be taken into consideration as a candidate of future networks modulation schemes.

REFERENCES

[1] Z. Ding, X. Lei, G. K. Karagiannidis, R. Schober, J. Yuan, and V. K. Bhargava, "A survey on non-orthogonal multiple access for 5g networks: Research challenges and future trends," *IEEE Journal on Selected Areas in Communications*, vol. 35, pp. 2181–2195, Oct 2017.

[2] L. Dai, B. Wang, Y. Yuan, S. Han, I. Chih-Lin, and Z. Wang, "Non-orthogonal multiple access for 5g: solutions, challenges, opportunities, and future research trends," *IEEE Communications Magazine*, vol. 53, pp. 74–81, 2015.

[3] Y. Saito, Y. Kishiyama, A. Benjebbour, T. Nakamura, A. Li, and K. Higuchi, "Non-orthogonal multiple access (noma) for cellular future radio access," in *2013 IEEE 77th Vehicular Technology Conference (VTC Spring)*, pp. 1–5, June 2013.

[4] B. Wang, K. Wang, Z. Lu, T. Xie, and J. Quan, "Comparison study of non-orthogonal multiple access schemes for 5g," in *2015 IEEE International Symposium on Broadband Multimedia Systems and Broadcasting*, pp. 1–5, June 2015.

[5] H. Mu, Z. Ma, M. Alhaji, P. Fan, and D. Chen, "A fixed low complexity message pass algorithm detector for up-link scma system," *IEEE Wireless Communications Letters*, vol. 4, pp. 585–588, Dec 2015.

[6] X. Dai, Z. Zhang, B. Bai, S. Chen, and S. Sun, "Pattern division multiple access: A new multiple access technology for 5g," *IEEE Wireless Communications*, vol. 25, pp. 54–60, April 2018.

[7] Çağrı Göken, A. Yılmaz, and O. Dizdar, "Evaluation of 5g new radio non-orthogonal multiple access methods for military applications," 2018.

[8] H. . Loeliger, "An introduction to factor graphs," *IEEE Signal Processing Magazine*, vol. 21, pp. 28–41, Jan 2004.

[9] F. R. Kschischang, B. J. Frey, and H. . Loeliger, "Factor graphs and the sum-product algorithm," *IEEE Transactions on Information Theory*, vol. 47, pp. 498–519, Feb 2001.

[10] A. Benjebbour and Y. Kishiyama, "Combination of noma and mimo: Concept and experimental trials," in *2018 25th International Conference on Telecommunications (ICT)*, pp. 433–438, 2018.

[11] E. G. Larsson, O. Edfors, F. Tufvesson, and T. L. Marzetta, "Massive mimo for next generation wireless systems," *IEEE Communications Magazine*, vol. 52, pp. 186–195, February 2014.

[12] E. Castañeda, A. Silva, A. Gameiro, and M. Kountouris, "An overview on resource allocation techniques for multi-user mimo systems," *IEEE Communications Surveys Tutorials*, vol. 19, pp. 239–284, Firstquarter 2017.

[13] J. Bao, Z. Ma, M. Xiao, Z. Ding, and Z. Zhu, "Performance analysis of uplink scma with receiver diversity and randomly deployed users," *IEEE Transactions on Vehicular Technology*, vol. 67, pp. 2792–2797, March 2018.

[14] A. O. Kalayci and G. M. Guvensen, "An efficient beam and channel acquisition via sparsity map and joint angle-delay power profile estimation for wideband massive mimo systems," 2019.

[15] A. Pitarokoilis, S. K. Mohammed, and E. G. Larsson, "On the optimality of single-carrier transmission in large-scale antenna systems," *IEEE Wireless Communications Letters*, vol. 1, pp. 276–279, August 2012.

[16] X. Song, S. Haghighatshoar, and G. Caire, "Efficient beam alignment for millimeter wave single-carrier systems with hybrid mimo transceivers," *IEEE Transactions on Wireless Communications*, vol. 18, pp. 1518–1533, March 2019.

[17] G. M. Guvensen and E. Ayanoglu, "A generalized framework on beamformer design and csi acquisition for single-carrier massive mimo systems in millimeter wave channels," in *2016 IEEE Globecom Workshops (GC Wkshps)*, pp. 1–7, Dec 2016.

[18] C. Dong, G. Gao, K. Niu, and J. Lin, "An efficient scma codebook optimization algorithm based on mutual information maximization," *Wireless Communications and Mobile Computing*, vol. 2018, pp. 1–13, 04 2018.

[19] M. Taherzadeh, H. Nikopour, A. Bayesteh, and H. Baligh, "Scma codebook design," in *2014 IEEE 80th Vehicular Technology Conference (VTC2014-Fall)*, pp. 1–5, Sep. 2014.

[20] K. Han, J. Hu, J. Chen, and H. Lu, "A low complexity sparse code multiple access detector based on stochastic computing," *IEEE Transactions on Circuits and Systems I: Regular Papers*, vol. 65, pp. 769–782, 2018.

[21] A. Goldsmith, *Wireless Communications*. New York, NY, USA: Cambridge University Press, 2005.

[22] X. Ma, L. Yang, Z. Chen, and Y. Siu, "Low complexity detection based on dynamic factor graph for scma systems," *IEEE Communications Letters*, vol. 21, pp. 2666–2669, Dec 2017.

[23] A. Lapidoth, "Mismatched decoding and the multiple access channel," in *Proceedings of 1994 IEEE International Symposium on Information Theory*, pp. 382–, June 1994.

[24] Z. Gülgün and A. . Yılmaz, "Detection schemes for high order m -ary qam under transmit nonlinearities," *IEEE Transactions on Communications*, vol. 67, pp. 4825–4834, July 2019.